The iron deficiency response of *Corynebacterium glutamicum* and a link to thiamine biosynthesis

Andreas Küberl, Aliye Mengus-Kaya, Tino Polen, and Michael Bott#

IBG-1: Biotechnology, Institute of Bio- and Geosciences, Forschungszentrum Jülich GmbH, 52425 Jülich, Germany

ORCID:	Andreas Küberl	orcid.org/0000-0001-9105-2452
ORCID:	Aliye Mengus-Kaya	orcid.org/0000-0002-9699-3048
ORCID:	Tino Polen	orcid.org/0000-0002-0065-3007
ORCID:	Michael Bott	orcid.org/0000-0002-4701-8254

#Corresponding author: m.bott@fz-juelich.de

Running title: Iron deficiency response of *Corynebacterium glutamicum*

Keywords: C*orynebacterium glutamicum*, iron deficiency, thiamine biosynthesis, transcriptome, proteome

A link has been created to allow review of the microarray data (GEO record GSE92397) while it remains in private status:
https://www.ncbi.nlm.nih.gov/geo/query/acc.cgi?token=ejsxucsulnwvzqj&acc=GSE92397
The mass spectrometry proteomics data have been deposited to the ProteomeXchange Consortium via the PRIDE partner repository with the dataset identifier PXD017349. For access at https://www.ebi.ac.uk/pride/archive log in with the username reviewer92838@ebi.ac.uk and the password Yh6ZHvQR.

ABSTRACT

The response to iron limitation of the Gram-positive soil bacterium *Corynebacterium glutamicum* was analyzed with respect to secreted metabolites, transcriptome, and proteome. During growth in glucose minimal medium, iron limitation caused a shift from lactate to pyruvate as major secreted organic acid complemented by L-alanine and 2-oxoglutarate. Transcriptome and proteome analyses revealed that a pronounced iron starvation response governed by the transcriptional regulators DtxR and RipA was detectable in the late, but not in the early exponential growth phase. A link between iron starvation and thiamine pyrophosphate (TPP) biosynthesis was uncovered by the strong upregulation of *thiC*. As phosphomethylpyrimidine synthase (ThiC) contains an iron-sulfur cluster, limiting activities of the TPP-dependent pyruvate/2-oxoglutarate dehydrogenase supercomplex probably cause the excretion of pyruvate and 2-oxoglutarate. In line with this explanation, thiamine supplementation could strongly diminish the secretion of these acids. The upregulation of *thiC* and other genes involved in thiamine biosynthesis and transport is presumably due to TPP riboswitches present at the 5'-end of the corresponding operons. The results obtained in this study provide new insights into iron homeostasis in *C. glutamicum* and demonstrate that the metabolic consequences of iron limitation can be due to the iron dependency of coenzyme biosynthesis.

IMPORTANCE

Iron is an essential element for most organisms, but causes problems due to poor solubility under oxic conditions and due to toxicity by catalyzing the formation of reactive oxygen species (ROS). Therefore, bacteria have evolved complex regulatory networks for iron homeostasis aiming at a sufficient iron supply while minimizing ROS formation. In our study the responses of the actinobacterium *Corynebacterium glutamicum* to iron limitation were analyzed, resulting in a detailed view on the processes involved in iron homeostasis in this model organism. In particular, we provide evidence that iron limitation causes TPP deficiency, presumably due to insufficient activity of the iron-dependent phosphomethylpyrimidine synthase (ThiC). TPP deficiency was deduced from upregulation of genes controlled by a TPP riboswitch and

secretion of metabolites caused by insufficient activity of the TPP-dependent enzymes pyruvate dehydrogenase and 2-oxoglutarate dehydrogenase. To our knowledge, the link between iron starvation and thiamine synthesis has not been elaborated previously.

INTRODUCTION

Iron is the fourth most abundant element in the Earth's crust (1). Based on its ability to exist in the ferrous (Fe^{2+}) and the ferric (Fe^{3+}) state, it has become a highly important constituent of many enzymes and is also discussed to be involved in the origin of life (2). In the form of iron centers, heme moieties, and iron–sulfur clusters, iron is crucial for the activity of many enzymes and regulatory proteins. Due to the very poor solubility of ferric iron that predominates under aerobic conditions, a sufficient supply of iron represents a considerable challenge for bacteria (3). However, not only an insufficient iron supply is problematic, but also excessive "free" iron within the cell, as in the presence of oxygen Fe^{2+} catalyzes the formation of reactive oxygen species (ROS) including the hydroxyl radical, which can damage virtually all organic molecules, such as proteins, DNA, and lipids (4). Therefore, bacteria have established sophisticated regulatory networks and mechanisms to ensure iron homeostasis (3-6).

We have previously explored various aspects of iron homeostasis in *Corynebacterium glutamicum*, an intensively studied Gram-positive soil bacterium of the *Actinobacteria* (7). This species possesses a large arsenal of genes devoted to iron uptake, including several ABC transporters for ferric siderophores or heme and several cytosolic siderophore-interacting proteins. However, *C. glutamicum* most likely does not produce siderophores on its own, but makes use of those produced by other bacteria (8). The majority of genes involved in iron uptake are members of the DtxR regulon. The transcriptional regulator DtxR (diphtheria toxin regulator) was characterized as master regulator controlling the expression of more than 50 genes involved in iron metabolism (9, 10). DtxR binds to its target promoters as a complex with ferrous iron and thus functions as a sensor of the cytosolic iron concentration (11). Besides the large set of genes encoding iron uptake systems, several target genes repressed by DtxR themselves encode transcriptional regulators, such as *ripA* and *hrrA*. The response regulator

HrrA is part of the HrrSA two-component system controlling the utilization of heme as an iron source (12-14). RipA (repressor of iron proteins) is an AraC-type transcriptional regulator repressing the expression of non-essential iron-dependent proteins, such as aconitase or succinate dehydrogenase, under low iron concentrations (15). RipA thereby ensures prolonged iron supply for essential iron-dependent proteins, such as ribonucleotide reductase, and thus has an analogous function as the small regulatory RNA RyhB in *Escherichia coli* (16).

Besides transcriptional regulation, we recently identified a posttranslational regulatory mechanism involved in iron homeostasis in *C. glutamicum* based on pupylation. Pupylation resembles eukaryotic ubiquitination and was initially identified in *Mycobacterium tuberculosis*, where pupylation usually tags proteins for degradation by the proteasome PrcAB (17, 18). *C. glutamicum* lacks a proteasome, but engages the ATPase ARC (called Mpa in mycobacteria) to unfold pupylated proteins. We found both ferritin and Dps to be subject to pupylation in *C. glutamicum*, with the small prokaryotic ubiquitin-like protein Pup covalently linked to Lys78 of ferritin and Lys14 of Dps (19). Ferritin pupylation was shown to be important for growth under iron limitation by enhancing the release of stored iron (20).

Despite the characterization of regulatory networks and mechanisms involved in iron homeostasis in *C. glutamicum*, knowledge about the physiological consequences of low iron availability and the dynamics of the response is still missing. Generally, it has been shown in bacteria that low iron concentrations result in a reduction of TCA cycle activity, lower energy production and, therefore, slowdown or even arrest of growth (21-24). Similar effects were observed also in eukaryotes such as the yeast *Saccharomyces cerevisiae*, where iron starvation increased the flux through glycolysis and diminished respiration as well as TCA cycle activity (25). In the present study, we aimed to obtain a detailed view of the iron starvation responses of *C. glutamicum* wild-type cells. For this purpose, we examined growth and the concomitant formation of metabolic by-products, and determined the iron starvation stimulon at the mRNA and protein level.

RESULTS

Influence of iron limitation on growth and by-product formation. We compared growth, pH, and by-product formation during shake flask cultivation of *C. glutamicum* in glucose minimal medium with either 1 µM $FeSO_4$ (iron limitation) or 36 µM $FeSO_4$ (iron sufficiency). The data obtained for various parameters are summarized in Table 1. In the cultivations with 222 mM glucose, we observed strong differences at different iron concentrations (Fig. 1). At 1 µM iron, the initial growth rates were only slightly lower compared to 36 µM iron, but the final OD_{600} was reduced by 57%, and 36 mM glucose remained unused. Cultures with 36 µM iron temporarily formed high concentrations of L-lactate (149 mM) and some acetate (14 mM), which were re-consumed when glucose became exhausted. Formation of L-lactate is a consequence of oxygen limitation at higher cell densities allowing the re-oxidation of NADH (26). Cultures supplemented with 1 µM iron instead of 36 µM, however, formed only small amounts of L-lactate (8 mM), but high concentrations of pyruvate (128 mM) and L-alanine (41 mM) as well as acetate (19 mM) and 2-oxoglutarate (6 mM). Neither the organic acids nor L-alanine were re-consumed. The pH of the cultures with 36 µM iron first dropped from pH 7 to about pH 6 due to the formation of the organic acids and then rose again up to pH 7 when the organic acids were re-consumed. In contrast, the pH of the cultures with 1 µM iron dropped to about pH 5 and remained there. The stronger acidification can be explained by the fact that pyruvic acid is a stronger acid (pK_a 2.49) than lactic acid (pK_a 3.90). The observation that the cells stopped consuming glucose and did not re-consume pyruvate, acetate, 2-oxoglutarate, and L-alanine suggests that the cells became metabolically inactive due to the acidification of the medium (27).

To test this assumption, we repeated the experiment with 111 mM glucose instead of 222 mM. In this case, the cultures grown at 1 µM iron consumed glucose completely and again formed pyruvate (32 mM), L-alanine (20 mM), acetate (8 mM), and 2-oxoglutarate (5 mM), but only minor levels of L-lactate (2 mM) (Fig. 2). Compared to the cultures with 222 mM glucose, the lower amount of acids formed presumably prevented critically strong acidification and pyruvate was slowly re-consumed after glucose depletion and partially converted to L-alanine.

141 This result supported the view that a low pH stopped metabolism in the cultivations with 222
142 mM glucose and 1 µM iron.
143
144 **Transcriptional responses to iron-limiting conditions.** It was previously shown by the
145 analysis of *C. glutamicum* Δ*dtxR* and Δ*ripA* mutants that DtxR and its subordinate regulator
146 RipA govern the iron starvation response of *C. glutamicum* (9, 10, 15). However, the temporal
147 onset of the transcriptional iron starvation response in the wild type of *C. glutamicum* is
148 unknown. Therefore, we performed two sets of DNA microarray experiments to compare the
149 mRNA levels of cells cultured under low and high iron conditions at different time points. In the
150 first set we analyzed the transcriptomes in the early exponential growth phase (OD_{600} = 4–5),
151 where cells grew comparably under low and high iron conditions (Fig. 1A). 51 genes showed
152 a ≥2-fold altered mRNA level with a *p*-value ≤0.05, of which 37 were up-regulated and 14
153 down-regulated (Table S1). Although the cells of the low iron culture had suffered from iron
154 limitation also during pre-cultivation, only four DtxR-regulated genes were slightly upregulated,
155 all of which presumably encode components of siderophore transporters (cg0769, cg0771,
156 cg0922, cg3404). The majority of DtxR targets, including the *ripA* gene, were unaltered. Most
157 of the genes with an increased mRNA level under iron limitation in the early exponential growth
158 phase were genes of the prophage CGP3 (23 of the totally 197 CGP3 prophage genes with
159 an average mRNA ratio of 3.5). In conclusion, at the chosen time point, the cells of the low iron
160 culture did not yet severely suffer from iron limitation.
161 In a second set of DNA microarray experiments, we compared transcript levels in the late
162 exponential growth phase (OD_{600} = 12-15), when the growth curves of the cultures with 36 µM
163 $FeSO_4$ and 1 µM $FeSO_4$ diverged and the first minute amounts of pyruvate were secreted by
164 the iron-depleted cells (Fig. 1A, D). At this time point the overall changes were much broader,
165 with in total 273 genes showing a ≥2-fold altered mRNA level with a *p*-value ≤0.05. 139 genes
166 were up-regulated, 134 genes down-regulated (Table S2). A strong iron starvation response
167 was observed, as 37 of the most strongly upregulated genes belong to the DtxR regulon and
168 17 of the most strongly downregulated genes represent all known members of the RipA regulon

(Table S2). The vast majority of upregulated DtxR target genes at this time point encode proteins involved in iron and heme uptake. These include three ABC transporters presumably catalyzing siderophore uptake (cg0589-cg0590-cg0591, cg0768-cg0769-cg0770, and cg0926-cg0927-cg0928), eight secreted siderophore-binding lipoproteins (cg0405, cg0748, cg0771, cg0922, cg0924, cg1418, cg2234, and cg3404), and three cytosolic siderophore-interacting proteins (cg0767, cg0921, and cg1405). The upregulated genes involved in heme uptake and utilization comprise one ABC transporter with a secreted heme-binding lipoprotein (cg0467-cg0468-cg0469), four secreted heme transport-associated proteins (cg0466, cg0470, cg0471, and cg3156), and heme oxygenase (cg2445). A number of genes reported to be repressed by DtxR were unaltered in our experiment, such as cg0955, cg1996-cg1998 (*cglIM-cglIR-cglIIR*), cg3082-cg3083, cg3084-cg3085, cg3112-cg3118 (*cysZYMDHXI*), and cg3119 (*cysJ*) (10). Various reasons can be responsible for the missing de-repression of these genes that are not directly involved in iron uptake, such as control by additional regulators or generally weak repression by DtxR.

Among the DtxR target genes encoding transcriptional regulators, *ripA* showed the highest upregulation with an mRNA ratio of 26 followed by *glyR* with a ratio of 8 and *hrrA* (not listed in Table S2) with a ratio of 1.9. With respect to the targets of these regulators, only those of RipA showed significantly altered expression. All 17 genes of the RipA regulon, most of which encode iron-containing proteins such as aconitase or succinate dehydrogenase, showed strongly reduced expression (Table S2). We assume that RipA economizes iron consumption under iron limitation by reducing the synthesis of non-essential iron-containing proteins, thereby prolonging the availability of iron for essential iron-dependent enzymes, such as ribonucleotide reductase.

Apart from members of the DtxR regulon (37 genes) and the RipA regulon (17 genes), 32 genes of the prophage CGP3 showed increased mRNA levels (on average 2.6-fold) (Table S2), similar to the results of the transcriptome comparison in the early exponential growth phase. A large functional group with altered expression under iron limitation was formed by 46 genes involved in transport, of which 28 were downregulated and 18 upregulated. The most

strongly downregulated operon was formed by cg0508-cg0507-cg0506 encoding an ABC transporter with similarity to the SfuABC Fe^{3+}-ABC transporter of *Serratia marcescens* (28). This transporter might have a lower affinity for Fe^{3+} and therefore could be relevant under iron-sufficient conditions. A putative thiamine-regulated ABC transporter for thiamine (cg1727-cg1728-cg1729, 3-fold increased expression), a putative Na^{+}-dependent secondary transporter of the BASS family (cg1419, 5-fold increased expression), and a putative dipeptide ABC transporter (cg2675-cg2676-cg2677-cg2678, 4-fold increased expression) were the most strongly upregulated transporter genes.

Another noticeable functional group with altered expression under iron limitation was formed by genes involved in respiration (29). All genes (*ctaD*, *ctaCF*, *ctaE-qcrCAB*) encoding the cytochrome bc_1-aa_3 supercomplex (30, 31) and one of the genes encoding the alternative cytochrome *bd* oxidase (32) showed 2- to 3-fold decreased expression under iron limitation. The regulators responsible for this effect are not yet known. Previous studies have demonstrated that the cAMP-dependent global regulator GlxR activates expression of the cytochrome bc_1-aa_3 supercomplex genes (33) and might be involved in the reduced expression observed in our experiment.

Among the very heterogeneous functional group of genes involved in carbon metabolism that showed altered expression under iron limitation, the most strongly regulated ones were *prpD2-prpB2-prpC2*, whose mRNA level was more than 7-fold decreased. They encode 2-methylcitrate dehydratase, 2-methylisocitrate lyase, and 2-methylcitrate synthase, key enzymes of the methylcitrate cycle involved in metabolization of propionate and propionyl-CoA derived from β-oxidation of odd-numbered fatty acids (34). This operon is transcriptionally regulated by several regulators including PrpR (35), RamA (36), and GlxR (37), allowing responses to various environmental stimuli. Among the group of genes involved in cofactor biosynthesis, the *thiC* gene encoding phosphomethylpyrimidine synthase was 8-fold upregulated and three additional genes involved in thiamine biosynthesis about 2-fold (*thiO*, *thiS*, *thiF*). This suggested that iron limitation might lead to thiamine deficiency (see below).

Among the group of further genes with altered expression under iron limitation, cg2962 was highly upregulated (12-fold, Table S2). Sequence analysis of Cg2962 revealed similarity to the heme oxygenases HmoA and HmoB of *Bacillus subtilis* and the *hmoA* and *hmoB* genes are repressed by the transcriptional regulator Fur under iron sufficiency (38-40). Since cg2962 was also >10-fold up-regulated in a Δ*dtxR* mutant compared to the wild type (Brune et al., 2006), we speculated that it might be another member of the DtxR regulon. Manual inspection of the promoter region indeed revealed a putative DtxR-binding motif (TGTAGTTAGGTTACACTAA), which was located between position -23 to -5 relative to the transcriptional start site of cg2962 (41), in agreement with a repressor function of DtxR. This binding site was probably not detected before because it contains six mismatches compared to the consensus DNA-binding motif of DtxR (TWAGGTWAGSCTWACCTWA). The results suggest that Cg2962 is another member of the DtxR regulon and might function as heme-degrading monooxygenase in *C. glutamicum* besides HmuO (Cg2445).

Relative protein level changes correlate with the mRNA level changes. Complementary to the transcriptome analysis, we also analyzed changes at the protein level for *C. glutamicum* cells grown at high and low iron concentrations and harvested in the late exponential growth phase. Between 1056 and 1357 proteins were detected (1% false discovery rate, FDR) in the 12 measurements (three biological replicates and two technical replicates each for low and high iron conditions) with a proteomic shotgun analysis using nanoLC-MS/MS, covering in total 1555 proteins (Table S3). By SWATH-MS measurements, relative levels of 1123 proteins could be quantified (Table S4). Thereof, 66 proteins exhibited at least two-fold altered ratios with a *p*-value ≤0.05 in iron-deprived cells compared to the cells cultivated with 36 µM iron. 38 proteins showed a ≥2-fold higher level under iron limitation, 16 of which were members of the DtxR regulon (Table S5). The levels of 28 proteins were at least 2-fold lower under iron limitation, 10 of which were members of the RipA regulon. In Table 2, the mRNA and protein ratios of the members of the DtxR and RipA regulon are summarized,

showing that the proteome data corroborate the transcriptome data. For the entire data sets, there was a good correlation between mRNA ratios and protein ratios (Fig. 3).

A link between iron deficiency and thiamine biosynthesis. Among the genes strongly upregulated under iron limitation was *thiC* (cg1476) encoding phosphomethylpyrimidine synthase, an enzyme involved in thiamine biosynthesis (Tables S2 and S5). Additional genes required for thiamine synthesis (*thiO*, *thiS*, *thiF*) and genes coding for a putative ABC transporter for thiamine (*ykoEDC*) were also ≥2-fold upregulated, although not as strong as *thiC*. These results suggested that *C. glutamicum* might face a shortage of thiamine pyrophosphate (TPP) under iron limitation. TPP shortage may result from an insufficient activity of ThiC, as the activity of this enzyme is dependent on an iron-sulfur center (42, 43). Considering that pyruvate and 2-oxoglutarate are oxidized by the TPP-dependent enzyme complexes pyruvate dehydrogenase (PDH) and 2-oxoglutarate dehydrogenase (ODH), the excretion of large amounts of pyruvate and smaller amounts of 2-oxoglutarate by *C. glutamicum* under iron limitation might be caused by limiting activities of these enzymes. To test this idea, we monitored the effect of thiamine addition (0.6 µM) on growth and by-product formation during cultivation in CGXII medium with 111 mM glucose and 1 µM $FeSO_4$. Supplementation of the medium with 0.6 µM thiamine significantly altered the pattern of secreted products after six hours (Fig. 2). Growth was slightly improved and the secretion of pyruvate, 2-oxoglutarate and L-alanine was reduced by approximately 50%, whereas the formation of acetate and lactate was slightly increased. These changes support the assumed TPP shortage under iron limitation.

DISCUSSION

In the present study, we have characterized the responses of the soil bacterium *C. glutamicum* to iron limitation with respect to growth, secreted metabolites, and changes in global mRNA and protein profiles. The combination of these results provides a detailed view

278 of the iron starvation response in *C. glutamicum* and revealed a link to thiamine biosynthesis
279 that may exist also in other microbes.

280 The transcriptome results obtained for cells cultivated with 1 µM iron and harvested in the
281 early exponential growth phase (OD_{600} = 4-5) revealed that only six DtxR-repressed genes
282 encoding components of siderophore ABC transporters were slightly derepressed (2- to 3-fold)
283 and none of the RipA target genes was repressed (Table S1). A more pronounced iron
284 starvation response might have been hindered by an initial accumulation of the available iron
285 within the cells. Whereas the iron starvation response was moderate, many CGP3 prophage
286 genes were upregulated under iron limitation in the early exponential growth phase. In a
287 previous study, elevated mRNA levels of CGP3 genes were observed in a Δ*dtxR* mutant (9).
288 This was explained by an increased excision of CGP3 from the genome and formation of
289 multiple circular CGP3 molecules, possibly triggered by DNA damage caused by elevated
290 intracellular iron concentrations (44). Induction of the prophage was also observed in the wild
291 type, but only in a small fraction of the population (44). The two-fold increase of several CGP3
292 genes observed in the early exponential growth phase of iron-starved cells may be due to
293 prophage induction in a minor fraction of the population. The exact mechanism connecting the
294 iron starvation response and CGP3 prophage induction remains to be elucidated.

295 In contrast to the moderate effects at an OD_{600} of 4-5, we observed a strong iron starvation
296 response at an OD_{600} of 12-15. Transcriptomics revealed that 37 of the known DtxR target
297 genes were strongly upregulated and 16 of the known RipA targets were 5- to 10-fold
298 downregulated (Table 2, Fig. 3). We could confirm altered expression of many of these genes
299 also at the protein level using a SWATH-MS approach (45). The transcriptome and proteome
300 data clearly indicate that a large fraction of DtxR was present in the apo-form dissociated from
301 its DNA targets at this time point. Besides known members of the DtxR regulon, we identified
302 a new one, cg2962, which encodes a putative heme monooxygenase based on sequence
303 similarity to the HmoA and HmoB proteins of *B. subtilis*. The position of the DtxR-binding site
304 upstream of cg2962 agrees with repression by DtxR.

The strong repression of the RipA target genes in the late exponential phase matches the strong upregulation of RipA (26-fold at the mRNA-level, 9-fold at the protein level). Currently, no mechanisms of activity control other than transcriptional repression by DtxR are known for RipA. In the case of the response regulator HrrA, which exhibited an only 2-fold increased mRNA level under iron limitation, transcriptional control of its target genes requires HrrA phosphorylation by the histidine kinase HrrS, which senses the presence of external heme (13, 14). As heme was not added in our experiments, HrrS presumably remained active as a phosphatase, preventing transcriptional regulation by HrrA. GlyR, another transcriptional regulator repressed by DtxR, was reported to activate expression of the *glyA* gene encoding serine hydroxymethyltransferase in the stationary phase (46). Although an 8-fold increased mRNA level and a 2-fold increased protein level of GlyR was detected in the late exponential phase of iron starvation, the *glyA* mRNA level remained unchanged, possibly because the cells had not yet entered the stationary phase. In summary, our data reveal the global iron starvation response of *C. glutamicum* wild type, which is in excellent agreement with the results obtained previously by transcriptome analysis of the deletion mutants Δ*dtxR* (9, 10) and Δ*ripA* (15). In a recent study, the iron starvation response of *Corynebacterium pseudotuberculosis* was analyzed by comparing global gene expression of cultures grown in the presence and absence of the iron chelator 2,2′-dipyridyl (47). The results obtained for the pathogenic *C. pseudotuberculosis* show many similarities to those obtained by us for the non-pathogenic *C. glutamicum*, such as upregulation of *ripA*, *hrrA*, and genes involved in heme utilization.

In the present study, we observed major differences between iron sufficiency and iron limitation with respect to the by-products secreted into the medium. Under iron sufficiency, cultivation in shake flasks with glucose minimal medium is typically associated with the transient formation of L-lactate, which is a consequence of oxygen limitation at higher cell densities and allows re-oxidation of NADH (26). Under iron limitation, however, high concentrations of pyruvate and L-alanine were formed instead of lactate accompanied by small amounts of 2-oxoglutarate (Figs. 1 and 2, Table 1). This indicates that the cells were not limited in oxygen but something else. Pyruvate is usually oxidized to acetyl-CoA and CO_2 by the

pyruvate dehydrogenase complex (48). In addition, pyruvate can be oxidized to acetate by pyruvate:quinone oxidoreductase (49). 2-Oxoglutarate is oxidized to succinyl-CoA and CO_2 by the 2-oxoglutarate dehydrogenase complex (50), which in *C. glutamicum* probably forms a supercomplex with the pyruvate dehydrogenase complex (51, 52). None of these enzymes is known to require iron for activity or to be repressed under iron limitation.

However, the analysis of the transcriptome and proteome data hinted to a different link between these enzymes and iron starvation. Cells harvested in the late exponential growth phase showed an 8-fold increased mRNA level of *thiC* and 2-fold increased mRNA levels of *thiO*, *thiS*, and *thiF*, all of which are involved in thiamine biosynthesis. The *thiC* gene encodes phosphomethylpyrimidine synthase (EC 4.1.99.17), an enzyme involved in TPP biosynthesis that catalyzes the conversion of 5-amino-1-(5-phospho-D-ribosyl)imidazole and S-adenosyl-L-methionine to 4-amino-2-methyl-5-(phosphooxymethyl)pyrimidine, 5'-deoxyadenosine, L-methionine, formate, and carbon monoxide. ThiC contains a [4Fe-4S] cluster to which its activity is strictly dependent on (42, 43, 53). Consequently, iron limitation may reduce ThiC activity and thus lead to a limitation in TPP.

TPP is a coenzyme of several enzymes with important roles in cellular metabolism (54). In *C. glutamicum*, these are for example the E1 subunit of the pyruvate dehydrogenase complex (Cg2466, AceE), the unusual E1 subunit of the 2-oxoglutarate dehydrogenase complex (Cg1280, OdhA), transketolase (Cg1774), pyruvate:menaquinone oxidoreductase (Cg2891), 1-deoxyxylulose-5-phosphate synthase (Cg2083), or acetolactate synthase (Cg1435). We could support the assumption that secretion of pyruvate and 2-oxoglutarate under iron limitation was a consequence of TPP limitation by the fact that thiamine supplementation reduced formation of these by-products. In addition, the observation that only L-alanine was secreted under iron limitation, but not L-valine, whereas both amino acids were produced by a mutant lacking the E1 subunit of the PDH complex (55), can be explained by a limiting activity of the TPP-dependent acetolactate synthase. In summary, our results suggest that iron limitation can lead to TPP limitation resulting in reduced activities of TPP-dependent enzymes when cells are dependent on endogenous TPP biosynthesis due to a lack of

exogenous thiamine or precursors thereof. This link between iron limitation and TPP biosynthesis probably exists not only in *C. glutamicum*, but also in other microbes. In *Bacillus licheniformis*, for example, the *tenA-thiVWX* operon encoding a protein (TenA) whose function is ambiguous and an ABC transporter for thiamine was reported to be up-regulated 2- to 3-fold under iron starvation (56). Interestingly, expression of the *pdhABCD* operon encoding the subunits of the pyruvate dehydrogenase complex was also up-regulated in *B. licheniformis* under these conditions, potentially as a consequence of a limiting TPP availability.

As *thiC* and the other thiamine biosynthesis genes are not members of the DtxR regulon, their upregulation under iron limitation must be due to expression control by a different transcriptional regulator or by a different mechanism. Comprehensive studies in the past years revealed that expression of TPP biosynthesis and thiamine transport genes in bacteria, but also in archaea and eukaryotes, is regulated by a riboswitch rather than by proteins (57-59). When sufficient TPP is available in the cell, it binds to the riboswitch located at the 5'-end of specific mRNAs triggering structural changes that either inhibit further transcription by forming a terminator or prevent translation initiation by blocking the ribosome binding site. Also both, transcription and translation, may be disturbed by formation of the riboswitch-TPP complex. In *E. coli* for example, the TPP riboswitch upstream of the *thiM* coding region inhibits translation, but not transcription, whereas the TPP riboswitch upstream of *thiC* inhibits both transcription and translation (58). In the genome of *C. glutamicum*, five TPP riboswitches were identified upstream of the coding sequences of *thiC* (cg1476), *thiM* (cg1655), *thiE* (cg2236), *ykoE* (cg1227), and cg0825 in bioinformatic studies (59, 60). The *ykoE* gene is the first gene of the *ykoE-ykoD-ykoC* operon presumably encoding a transporter for thiamine uptake (61). The *thiE* gene is the first gene of the *thiE-thiO-thiS-thiG-thiF* operon encoding enzymes involved in thiamine biosynthesis. The cg0825 gene has been annotated to encode a short chain dehydrogenase, but its function in thiamine biosynthesis is unknown. Based on the prediction of TPP riboswitches, we assume that the enhanced transcription under iron limitation of *thiC* and further genes involved in TPP biosynthesis or thiamine transport is caused by the TPP riboswitch as a consequence of TPP shortage due to insufficient activity of the iron-dependent

ThiC enzyme. Table 3 summarizes the mRNA and protein ratios under iron limitation of the genes predicted to be controlled by a TPP riboswitch in *C. glutamicum*. Except for *thiM*, upregulated mRNA and protein levels were observed for all of them, supporting the view that iron limitation caused TPP deficiency.

In Fig. 4, an overview on the currently known iron starvation responses of *C. glutamicum* is shown, including the findings presented in this study. The scheme depicts four major responses observed or relevant under iron-limiting conditions, *i.e.* the up-regulation of genes involved in iron and heme acquisition, the down-regulation of genes for non-essential proteins requiring iron, the pupylation of ferritin and Dps to release stored iron, and the consequences of thiamine limitation on central metabolism. Despite these features already uncovered, there are still many aspects missing in our understanding of the iron starvation response of *C. glutamicum*, such as the substrates and relevance of the different siderophore transporters, the temporal order of induction of the iron starvation genes, or the hierarchy of iron delivery to iron-dependent enzymes.

MATERIALS AND METHODS

Strains and cultivation conditions. The *C. glutamicum* type strain ATCC 13032 served as wild type in the present study. Cultivation was performed in CGXII minimal medium containing 111 mM or 222 mM glucose as main carbon and energy source and 195 µM protocatechuic acid as iron chelator (62). To establish iron limiting conditions, the concentration of iron in the CGXII medium was reduced from 36 µM to 1 µM, as described previously (20). When indicated, thiamine hydrochloride was added to CGXII medium in a concentration of 0.6 µM using a 3 mM stock solution. Growth experiments were started with a first pre-culture in 5 ml Brain Heart Infusion (BHI) medium (Difco Laboratories) shaken for 8 h at 170 rpm. The second pre-culture in 20 ml CGXII minimal medium was inoculated using 500 µl of the first pre-culture and shaken overnight (16 h) at 140 rpm. The second pre-culture was used to inoculate the main culture in 50 ml CGXII medium to an optical density at 600 nm (OD_{600}) of 1 and growth was monitored using a spectrophotometer at 600 nm. For cultivation

under iron limitation, the cells were washed in 0.9% (wt/vol) NaCl solution before inoculating the next cultures.

Quantification of metabolites in culture supernatants by HPLC. The presence and concentration of organic acids, amino acids, and glucose in culture supernatants was determined using HPLC as described earlier (26, 63). Culture supernatants were diluted 1:4 (organic acids and glucose) or 1:100 (amino acids) in dH_2O and centrifuged for 5 min at 16,000 *g* before used for HPLC analysis.

Transcriptome analyses using DNA microarrays. For RNA extraction of *C. glutamicum* samples, cells were cultured in biological triplicates under low or high iron conditions and were harvested in the early (OD_{600} = 4 – 5) and late (OD_{600} = 12 – 15) exponential phase. Comparison of mRNA levels under these conditions was performed according to established protocols for RNA preparation, cDNA synthesis, hybridization, and data analysis (63). The microarray data have been deposited in the National Center for Biotechnology Information Gene Expression Omnibus (GEO) database and are available in GEO through accession numbers GSE92348 (early) and GSE92359 (late), or GSE92397 for both sets.

Sample preparation for proteome analyses. Cells were harvested in the late exponential growth phase (OD_{600} = 12 – 15) from biological triplicate cultures as for the DNA microarray experiments. Cell pellets were resuspended in 1.5 ml buffer (50 mM potassium phosphate, pH 8.0, 20 mM EDTA, 2 mM DTT, including Complete Mini protease inhibitor from Roche Diagnostics) and disrupted using a Precellys cell disruptor three time for 30 s at 6,500 rpm. Cell debris was removed by centrifugation (20 min at 16,000 *g* and 4°C). Protein concentrations of crude cell extracts were determined by a Bradford assay (64). For tryptic digestion, 50 µg of protein was treated with the Trypsin Singles Proteomics Grade Kit (Sigma-Aldrich) in a volume of 100 µl according to the manufacturer's instructions for solution digestion. Then 100 µl of 0.1% formic acid in HLPC-grade water was added and the samples

were subjected to ultrafiltration using Nanosep Centrifugal Devices with Omega membrane 10K (Pall) that were centrifuged at 16,100 *g* for 20 min at 4 °C to get rid of remaining particles, undigested proteins, and peptides larger than 10 kDa. The tryptic peptide samples were stored at −20°C until use for MS measurements.

Shotgun proteomic measurement. After tryptic digestion, the peptides were separated chromatographically on a nanoLC Eksigent ekspert™ 425 system (Sciex) coupled with a quartz emitter tip (New Objective) to a TripleTof™ 6600 mass spectrometer (Sciex) and measured as technical duplicate. Sample volumes of 3 µl containing 1.5 µg of digested protein were loaded on a pre-column (ChromXP C18-3 µm, 350 µm x 0.5 mm, Sciex) from the cooled (8°C) autosampler for desalting and enrichment using a flow of 3 µl/min (10 min) of buffer A (0.1% formic acid in HLPC-grade water). The separation of peptides followed on an analytical column (ChromXP 3C18-CL-120, 150 mm x 0.75 mm, Sciex) with a gradient method (125 min) using buffer A and buffer B (0.1% formic acid in acetonitrile) at 40 °C and a flow of 300 nl/min. The gradient conditions were 5% buffer B for 1 min, 5% - 9% for 9 min, 9% - 20% for 50 min, 20% - 40% for 40 min, 40% - 80% for 5 min, and 80% for 4 min. Before injection of the next sample, the column was equilibrated with 5% of buffer B for 16 min. For shotgun measurements by information dependent acquisition scanning (IDA) the mass spectrometer was operated with a “top 50” method: Initially, a 250 ms survey scan (TOF-MS mass range *m/z* 400 - 1500, high resolution mode) was collected, from which the top 50 precursor ions were automatically selected for fragmentation, whereby each MS/MS event (mass range *m/z* 100 - 1700, high sensitivity mode) consisted of a 75 ms fragment ion scan. The main selection criterion for parent ion selection was precursor ion intensity. Ions with an intensity exceeding 100 counts per second and a charge state of 2^+ to 5^+ were preferentially selected. Selected precursors were added to a dynamic exclusion list for 22 s. Precursor ions were isolated using a quadrupole resolution of 0.7 amu and fragmented in the collision cell with a rolling collision energy (CE) of 10. If less than 50 precursor ions fulfilling the selection criteria were detected per survey scan, the detected precursors were subjected to extended MS/MS accumulation

time to maintain a constant total cycle time of 4 s. The source and gas settings were 2200 V spray, 40 psi curtain gas, 6 psi ion source gas, and 75°C interface heater.

Proteomic analysis with SWATH–MS. For SWATH-based MS measurements optimized Q1 transmission windows were created for the *C. glutamicum* samples with the SWATH Variable Windows Calculator (V1.0, Sciex) as a set of 30 overlapping windows (1 amu overlap) covering the mass range *m/z* 200 – 1600 in high sensitivity mode. The rolling collision energy was selected with a charge state of 2+ and CE of 10. An accumulation time of 49.96 ms was used for each fragment ion scan and for the survey scan acquired at the beginning of each cycle, resulting in a total cycle time of 2.98 s. The source and gas settings were 2200 V spray, 40 psi curtain gas, 6 psi ion source gas, and 75°C interface heater. Each sample was measured as technical duplicate using the same gradient method as for IDA.

Data processing and statistical analysis. Our analysis aimed at the identification of proteins with significantly altered abundance in *C. glutamicum* between low and high iron conditions. The IDA data from both growth conditions were processed with ProteinPilot™ (V4.5 beta, Sciex) using the Paragon algorithm for peptide and protein identification to create a spectral library from *C. glutamicum* for the SWATH measurements. Using this library, the SWATH data were processed with PeakView® (V2.1, Sciex) to identify peptides (99% confidence) and proteins (1% FDR). Before quantification, retention time calibration between IDA and SWATH measurements were performed and applied to all peptides in the ion library using manually selected peptides with retention times to cover the complete time span of the gradient. For quantification using PeakView® the peptide process settings were set to 10 peptides per protein, 6 transitions per peptide, 99% peptide confidence threshold and 75 ppm XIC width. The list of proteins with quantified intensities was reduced to proteins detected in all samples. Then, the arithmetic mean of six peak areas per protein detected was calculated separately for both conditions. The six values arose from three biological replicates with two technical replicates each. The ratio of protein levels under iron limitation versus iron

sufficiency was calculated including a two-sided student's *t*-test to determine the *p*-value. Protein levels were considered significantly altered between the two conditions if they exhibited a fold change of >1.5 and a *p*-value ≤0.05.

Data availability. The microarray data have been deposited in the National Center for Biotechnology Information Gene Expression Omnibus (GEO) database and are accessible in GEO through the accession numbers GSE92348 (OD_{600} 4-5) and GSE92359 (OD_{600} 12-15), or GSE92397 for both sets. The mass spectrometry proteomics data have been deposited to the ProteomeXchange Consortium via the PRIDE partner repository with the dataset identifier PXD017349.

REFERENCES

1. Weber KA, Achenbach LA, Coates JD. 2006. Microorganisms pumping iron: anaerobic microbial iron oxidation and reduction. Nat Rev Microbiol 4:752-764.
2. Thiel J, Byrne JM, Kappler A, Schink B, Pester M. 2019. Pyrite formation from FeS and H_2S is mediated through microbial redox activity. Proc Natl Acad Sci USA 116:6897-6902.
3. Andrews SC, Robinson AK, Rodriguez-Quinones F. 2003. Bacterial iron homeostasis. FEMS Microbiol Rev 27:215-237.
4. Cornelis P, Wei Q, Andrews SC, Vinckx T. 2011. Iron homeostasis and management of oxidative stress response in bacteria. Metallomics 3:540-549.
5. Frawley ER, Fang FC. 2014. The ins and outs of bacterial iron metabolism. Mol Microbiol 93:609-816.
6. Rodriguez GM. 2006. Control of iron metabolism in *Mycobacterium tuberculosis*. Trends Microbiol 14:320-327.
7. Eggeling L, Bott M (ed). 2005. Handbook of *Corynebacterium glutamicum*. CRC Press, Taylor & Francis Group, Boca Raton, Florida, USA.
8. Frunzke J, Bott M. 2008. Regulation of iron homeostasis in *Corynebacterium glutamicum*, p 241-266. *In* Burkovski A (ed), Corynebacteria: Genomics and Molecular Biology. Caister Academic Press, Norfolk, UK.
9. Wennerhold J, Bott M. 2006. The DtxR regulon of *Corynebacterium glutamicum*. J Bacteriol 188:2907-2918.
10. Brune I, Werner H, Hüser AT, Kalinowski J, Pühler A, Tauch A. 2006. The DtxR protein acting as dual transcriptional regulator directs a global regulatory network involved in iron metabolism of *Corynebacterium glutamicum*. BMC Genomics 7:21.
11. White A, Ding X, vanderSpek JC, Murphy JR, Ringe D. 1998. Structure of the metal-ion-activated diphtheria toxin repressor/tox operator complex. Nature 394:502-506.
12. Frunzke J, Gätgens C, Brocker M, Bott M. 2011. Control of heme homeostasis in *Corynebacterium glutamicum* by the two-component system HrrSA. J Bacteriol 193:1212-1221.
13. Hentschel E, Mack C, Gätgens C, Bott M, Brocker M, Frunzke J. 2014. Phosphatase activity of the histidine kinases ensures pathway specificity of the ChrSA and HrrSA two-component systems in *Corynebacterium glutamicum*. Mol Microbiol 92:1326-1342.
14. Keppel M, Davoudi E, Gätgens C, Frunzke J. 2018. Membrane topology and heme binding of the histidine kinases HrrS and ChrS in *Corynebacterium glutamicum*. Front Microbiol 9:183.
15. Wennerhold J, Krug A, Bott M. 2005. The AraC-type regulator RipA represses aconitase and other iron proteins from *Corynebacterium* under iron limitation and is itself repressed by DtxR. J Biol Chem 280:40500-40508.

16. Masse E, Gottesman S. 2002. A small RNA regulates the expression of genes involved in iron metabolism in *Escherichia coli*. Proc Nat Acad Sci USA 99:4620-4625.
17. Pearce MJ, Mintseris J, Ferreyra J, Gygi SP, Darwin KH. 2008. Ubiquitin-like protein involved in the proteasome pathway of *Mycobacterium tuberculosis*. Science 322:1104-1107.
18. Striebel F, Imkamp F, Özcelik D, Weber-Ban E. 2014. Pupylation as a signal for proteasomal degradation in bacteria. Biochim Biophys Acta 1843:103-113.
19. Küberl A, Fränzel B, Eggeling L, Polen T, Wolters DA, Bott M. 2014. Pupylated proteins in *Corynebacterium glutamicum* revealed by MudPIT analysis. Proteomics 14:1531-1542.
20. Küberl A, Polen T, Bott M. 2016. The pupylation machinery is involved in iron homeostasis by targeting the iron storage protein ferritin. Proc Natl Acad Sci USA 113:4806-4811.
21. Smaldone GT, Revelles O, Gaballa A, Sauer U, Antelmann H, Helmann JD. 2012. A global investigation of the *Bacillus subtilis* iron-sparing response identifies major changes in metabolism. J Bacteriol 194:2594-2605.
22. Pieper R, Huang ST, Parmar PP, Clark DJ, Alami H, Fleischmann RD, Perry RD, Peterson SN. 2010. Proteomic analysis of iron acquisition, metabolic and regulatory responses of *Yersinia pestis* to iron starvation. BMC Microbiol 10:30.
23. Fourquez M, Devez A, Schaumann A, Gueneugues A, Jouenne T, Obernosterer I, Blain S. 2014. Effects of iron limitation on growth and carbon metabolism in oceanic and coastal heterotrophic bacteria. Limnol Oceanogr 59:349-360.
24. Folsom JP, Parker AE, Carlson RP. 2014. Physiological and proteomic analysis of *Escherichia coli* iron-limited chemostat growth. J Bacteriol 196:2748-2761.
25. Shakoury-Elizeh M, Protchenko O, Berger A, Cox J, Gable K, Dunn TM, Prinz WA, Bard M, Philpott CC. 2010. Metabolic response to iron deficiency in *Saccharomyces cerevisiae*. J Biol Chem 285:14823-14833.
26. Koch-Koerfges A, Kabus A, Ochrombel I, Marin K, Bott M. 2012. Physiology and global gene expression of a *Corynebacterium glutamicum* ΔF_1F_O-ATP synthase mutant devoid of oxidative phosphorylation. Biochim Biophys Acta 1817:370-380.
27. Follmann M, Ochrombel I, Krämer R, Trotschel C, Poetsch A, Rückert C, Hüser A, Persicke M, Seiferling D, Kalinowski J, Marin K. 2009. Functional genomics of pH homeostasis in *Corynebacterium glutamicum* revealed novel links between pH response, oxidative stress, iron homeostasis and methionine synthesis. BMC Genomics 10:621.
28. Angerer A, Klupp B, Braun V. 1992. Iron transport systems of *Serratia marcescens*. J Bacteriol 174:1378-1387.
29. Bott M, Niebisch A. 2003. The respiratory chain of *Corynebacterium glutamicum*. J Biotechnol 104:129-153.
30. Niebisch A, Bott M. 2001. Molecular analysis of the cytochrome bc_1-aa_3 branch of the *Corynebacterium glutamicum* respiratory chain containing an unusual diheme cytochrome c_1. Arch Microbiol 175:282-294.
31. Niebisch A, Bott M. 2003. Purification of a cytochrome bc_1-aa_3 supercomplex with quinol oxidase activity from *Corynebacterium glutamicum* - Identification of a fourth subunit of cytochrome aa_3 oxidase and mutational analysis of diheme cytochrome c_1. J Biol Chem 278:4339-4346.
32. Kusumoto K, Sakiyama M, Sakamoto J, Noguchi S, Sone N. 2000. Menaquinol oxidase activity and primary structure of cytochrome *bd* from the amino-acid fermenting bacterium *Corynebacterium glutamicum*. Arch Microbiol 173:390-397.
33. Toyoda K, Teramoto H, Inui M, Yukawa H. 2011. Genome-wide identification of *in vivo* binding sites of GlxR, a cyclic AMP receptor protein-type regulator in *Corynebacterium glutamicum*. J Bacteriol 193:4123-4133.
34. Bott M. 2007. Offering surprises: TCA cycle regulation in *Corynebacterium glutamicum*. Trends Microbiol 15:417-425.
35. Plassmeier J, Persicke M, Pühler A, Sterthoff C, Rückert C, Kalinowski J. 2012. Molecular characterization of PrpR, the transcriptional activator of propionate catabolism in *Corynebacterium glutamicum*. J Biotechnol 159:1-11.
36. Auchter M, Cramer A, Hüser A, Rückert C, Emer D, Schwarz P, Arndt A, Lange C, Kalinowski J, Wendisch VF, Eikmanns BJ. 2011. RamA and RamB are global transcriptional regulators in *Corynebacterium glutamicum* and control genes for enzymes of the central metabolism. J Biotechnol 154:126-139.
37. Jungwirth B, Sala C, Kohl TA, Uplekar S, Baumbach J, Cole ST, Pühler A, Tauch A. 2013. High-resolution detection of DNA binding sites of the global transcriptional regulator GlxR in *Corynebacterium glutamicum*. Microbiology 159:12-22.
38. Gaballa A, Helmann JD. 2011. *Bacillus subtilis* Fur represses one of two paralogous haem-degrading monooxygenases. Microbiology 157:3221-3231.

608 39. Park S, Kim D, Jang I, Oh HB, Choe J. 2014. Structural and biochemical study of *Bacillus subtilis*
609 HmoB in complex with heme. Biochem Biophys Res Commun 446:286-291.
610 40. Park S, Choi S, Choe J. 2012. *Bacillus subtilis* HmoB is a heme oxygenase with a novel structure.
611 BMB Rep 45:239-241.
612 41. Pfeifer-Sancar K, Mentz A, Rückert C, Kalinowski J. 2013. Comprehensive analysis of the
613 *Corynebacterium glutamicum* transcriptome using an improved RNAseq technique. BMC
614 Genomics 14:888.
615 42. Chatterjee A, Li Y, Zhang Y, Grove TL, Lee M, Krebs C, Booker SJ, Begley TP, Ealick SE. 2008.
616 Reconstitution of ThiC in thiamine pyrimidine biosynthesis expands the radical SAM superfamily.
617 Nat Chem Biol 4:758-765.
618 43. Martinez-Gomez NC, Downs DM. 2008. ThiC is an [Fe-S] cluster protein that requires AdoMet to
619 generate the 4-amino-5-hydroxymethyl-2-methylpyrimidine moiety in thiamin synthesis.
620 Biochemistry 47:9054-9060.
621 44. Frunzke J, Bramkamp M, Schweitzer JE, Bott M. 2008. Population heterogeneity in
622 *Corynebacterium glutamicum* ATCC 13032 caused by prophage CGP3. J Bacteriol 190:5111-
623 5119.
624 45. Gillet LC, Navarro P, Tate S, Rost H, Selevsek N, Reiter L, Bonner R, Aebersold R. 2012.
625 Targeted data extraction of the MS/MS spectra generated by data-independent acquisition: a new
626 concept for consistent and accurate proteome analysis. Mol Cell Proteomics 11:1-17.
627 46. Schweitzer JE, Stolz M, Diesveld R, Etterich H, Eggeling L. 2009. The serine
628 hydroxymethyltransferase gene *glyA* in *Corynebacterium glutamicum* is controlled by GlyR. J
629 Biotechnol 139:214-21.
630 47. Ibraim IC, Parise MTD, Parise D, Sfeir MZT, de Paula Castro TL, Wattam AR, Ghosh P, Barh D,
631 Souza EM, Goes-Neto A, Gomide ACP, Azevedo V. 2019. Transcriptome profile of
632 *Corynebacterium pseudotuberculosis* in response to iron limitation. BMC Genomics 20:663.
633 48. Schreiner ME, Fiur D, Holatko J, Patek M, Eikmanns B. 2005. E1 enzyme of the pyruvate
634 dehydrogenase complex in *Corynebacterium glutamicum*: molecular analysis of the gene and
635 phylogenetic aspects. J Bacteriol 187:6005-6018.
636 49. Schreiner ME, Eikmanns BJ. 2005. Pyruvate:quinone oxidoreductase from *Corynebacterium*
637 *glutamicum*: Purification and biochemical characterization. J Bacteriol 187:862-871.
638 50. Usuda Y, Tujimoto N, Abe C, Asakura Y, Kimura E, Kawahara Y, Kurahashi O, Matsui H. 1996.
639 Molecular cloning of the *Corynebacterium glutamicum* ('*Brevibacterium lactofermentum*'
640 AJ12036) *odhA* gene encoding a novel type of 2-oxoglutarate dehydrogenase. Microbiology
641 142:3347-3354.
642 51. Hoffelder M, Raasch K, van Ooyen J, Eggeling L. 2010. The E2 domain of OdhA of
643 *Corynebacterium glutamicum* has succinyltransferase activity dependent on lipoyl residues of the
644 acetyltransferase AceF. J Bacteriol 192:5203-5211.
645 52. Niebisch A, Kabus A, Schultz C, Weil B, Bott M. 2006. Corynebacterial protein kinase G controls
646 2-oxoglutarate dehydrogenase activity via the phosphorylation status of the OdhI protein. J Biol
647 Chem 281:12300-12307.
648 53. Dougherty MJ, Downs DM. 2006. A connection between iron-sulfur cluster metabolism and the
649 biosynthesis of 4-amino-5-hydroxymethyl-2-methylpyrimidine pyrophosphate in *Salmonella*
650 *enterica*. Microbiology 152:2345-2353.
651 54. Bunik VI, Tylicki A, Lukashev NV. 2013. Thiamin diphosphate-dependent enzymes: from
652 enzymology to metabolic regulation, drug design and disease models. FEBS J 280:6412-6442.
653 55. Blombach B, Schreiner ME, Holatko J, Bartek T, Oldiges M, Eikmanns BJ. 2007. L-valine
654 production with pyruvate dehydrogenase complex-deficient *Corynebacterium glutamicum*. Appl
655 Environ Microbiol 73:2079-2084.
656 56. Nielsen AK, Breuner A, Krzystanek M, Andersen JT, Poulsen TA, Olsen PB, Mijakovic I,
657 Rasmussen MD. 2010. Global transcriptional analysis of *Bacillus licheniformis* reveals an overlap
658 between heat shock and iron limitation stimulon. J Mol Microbiol Biotechnol 18:162-173.
659 57. Miranda-Rios J, Navarro M, Soberon M. 2001. A conserved RNA structure (thi box) is involved in
660 regulation of thiamin biosynthetic gene expression in bacteria. Proc Natl Acad Sci U S A 98:9736-
661 41.
662 58. Winkler W, Nahvi A, Breaker RR. 2002. Thiamine derivatives bind messenger RNAs directly to
663 regulate bacterial gene expression. Nature 419:952-956.
664 59. Rodionov DA, Vitreschak AG, Mironov AA, Gelfand MS. 2002. Comparative genomics of thiamin
665 biosynthesis in procaryotes. New genes and regulatory mechanisms. J Biol Chem 277:48949-
666 48959.

60. Mentz A, Neshat A, Pfeifer-Sancar K, Pühler A, Rückert C, Kalinowski J. 2013. Comprehensive discovery and characterization of small RNAs in *Corynebacterium glutamicum* ATCC 13032. BMC Genomics 14:714.
61. Josts I, Almeida Hernandez Y, Andreeva A, Tidow H. 2016. Crystal structure of a group I energy coupling factor vitamin transporter S component in complex with its cognate substrate. Cell Chem Biol 23:827-836.
62. Frunzke J, Engels V, Hasenbein S, Gätgens C, Bott M. 2008. Co-ordinated regulation of gluconate catabolism and glucose uptake in *Corynebacterium glutamicum* by two functionally equivalent transcriptional regulators, GntR1 and GntR2. Mol Microbiol 67:305-322.
63. Vogt M, Haas S, Klaffl S, Polen T, Eggeling L, van Ooyen J, Bott M. 2014. Pushing product formation to its limit: Metabolic engineering of *Corynebacterium glutamicum* for L-leucine overproduction. Metab Eng 22:40-52.
64. Bradford MM. 1976. A rapid and sensitive method for the quantitation of microgram quantities of protein utilizing the principle of protein-dye binding. Anal Biochem 72:248-254.

Table 1. Growth parameters, pH, specific glucose uptake rates (sGUR), and concentrations of organic and amino acids in supernatants of *C. glutamicum* cultures grown in CGXII medium with 111 mM glucose or 222 mM glucose either under iron sufficiency (36 µM $FeSO_4$) or under iron limitation (1 µM).

Parameter[1,2]	**111 mM glucose, 36 µM Fe**	**111 mM glucose, 1 µM Fe**	**222 mM glucose, 36 µM Fe**	**222 mM glucose, 1 µM Fe**
Final OD_{600}	32 ± 2	21 ± 1	63 ± 12	27 ± 1
µ (h^{-1})	0.44 ± 0.01	0.39 ± 0.03	0.40 ± 0.01	0.37 ± 0.00
pH $value_{max}$	7.7 ± 0.0	7.6 ± 0.0	7.5 ± 0.1	7.5 ± 0.1
pH $value_{min}$	7.0 ± 0.0	7.0 ± 0.0	5.9 ± 0.1	4.9 ± 0.1
sGUR (nmol min^{-1} (mg CDW)$^{-1}$)	93.7 ± 4.3	72.1 ± 6.4	89.0 ± 0.6	50.9 ± 0.5
Final glucose conc., 48 h (mM)	0	0	0	36.1 ± 1.8
$Acetate_{max}$ (mM)	5.44 ± 2.61	7.68 ± 1.09	14.4 ± 4.7	18.5 ± 0.6
$Acetate_{max}$ (mmol (g CDW)$^{-1}$)	0.74 ± 0.38	1.64 ± 0.42	0.74 ± 0.50	2.79 ± 0.14
$Lactate_{max}$ (mM)	31.9 ± 6.6	1.94 ± 0.11	149 ± 31	8.32 ± 0.86
$Lactate_{max}$ (mmol (g CDW)$^{-1}$)	4.29 ± 1.12	0.46 ± 0.04	13.0 ± 5.0	1.25 ± 0.11
$Pyruvate_{max}$ (mM)	<1	32.4 ± 2.7	<1	128.0 ± 0.6
$Pyruvate_{max}$ (mmol (g CDW)$^{-1}$)	<1	6.84 ± 0.37	<1	19.0 ± 1.3
2-$Oxoglutarate_{max}$ (mM)	<1	5.44 ± 0.17	<1	6.37 ± 0.12
2-$Oxoglutarate_{max}$ (mmol (g CDW)$^{-1}$)	<1	1.24 ± 0.11	<1	0.94 ± 0.01
$Alanine_{max}$ (mM)	<1	19.8 ± 2.7	<1	40.8 ± 0.3
$Alanine_{max}$ (mmol (g CDW)$^{-1}$)	<1	4.37 ± 0.73	<1	6.3 ± 0.0

[1]For all parameters mean values and standard deviations derived from three independent biological replicates are given. Maximum concentrations of organic and amino acids in supernatants are shown as absolute values and relative to cell dry weight (CDW).
[2]Values for growth with 222 mM glucose and 36 µM Fe were taken from (26).

Table 2. mRNA ratios and protein ratios under low and high iron conditions of the genes and proteins transcriptionally regulated by DtxR and RipA in *C. glutamicum*.[1]

Gene locus	Gene name	Annotation	Early: mRNA ratio low/high Fe	Late: mRNA ratio low/high Fe	Late: protein ratio low/high Fe
		DtxR regulon			
cg0160		hypothetical protein	1.06	**10.95**	n.d.
cg0405		putative ferric dicitrate ABC transporter, secreted siderophore-binding lipoprotein	1.24	**10.05**	**11.95**
cg0465		putative membrane protein, conserved	1.52	**10.22**	n.d.
cg0466	*htaA*	secreted heme transport-associated protein	1.61	**11.93**	n.d.
cg0467	*hmuT*	heme ABC transporter, secreted heme-binding lipoprotein	1.26	**8.83**	**1.82**
cg0468	*hmuU*	heme ABC transporter, permease	1.18	**7.28**	n.d.
cg0469	*hmuV*	heme ABC transporter, ATPase	0.84	**4.27**	n.d.
cg0470	*htaB*	secreted heme transport-associated protein	1.09	**118.62**	**5.17**
cg0471	*htaC*	secreted heme transport-associated protein	0.62	**53.40**	0.75
cg0527	*glyR*	ArsR-type transcriptional regulator of *glyA*	1.07	**7.89**	1.80
cg0589		putative siderophore ABC transporter, ATPase	1.87	**9.69**	1.39
cg0590		putative siderophore ABC transporter, permease	1.88	**11.39**	**9.58**
cg0591		putative siderophore ABC transporter, permease	1.34	**5.94**	n.d.
cg0748		putative siderophore ABC transporter, secreted substrate-binding lipoprotein	1.07	**4.93**	**6.70**
cg0767		putative cytoplasmic siderophore-interacting protein	1.12	**7.25**	**5.36**
cg0768		putative siderophore ABC transporter, ATPase	1.83	**10.01**	1.14
cg0769		putative siderophore ABC transporter, permease	**2.77**	**6.87**	n.d.
cg0770		putative siderophore ABC transporter, permease	1.50	**10.28**	n.d.
cg0771	*irp1*	putative siderophore ABC transporter, secreted siderophore-binding lipoprotein	**2.20**	**12.77**	**6.18**
cg0921		putative cytoplasmic siderophore-interacting protein	1.12	**14.81**	n.d.
cg0922		putative secreted siderophore-binding lipoprotein	**2.20**	**19.62**	**4.87**
cg0924		putative siderophore ABC transporter, secreted substrate-binding lipoprotein	2.12	**12.97**	**9.29**
cg0926		putative siderophore ABC transporter, permease	1.90	**6.42**	n.d.
cg0927		putative siderophore ABC transporter, permease	**2.08**	**8.81**	1.25
cg0928		putative siderophore ABC transporter, ATPase	1.32	**4.30**	**4.23**
cg1120	*ripA*	AraC family transcriptional regulator of iron proteins	1.42	**25.83**	**9.14**
cg1405		putative cytoplasmic siderophore-interacting protein	1.02	**6.63**	**2.69**
cg1418		putative secreted siderophore-binding lipoprotein	1.39	**7.94**	**3.49**
cg1930		putative secreted hydrolase, CGP3 region	1.36	**34.35**	0.86
cg1931		putative secreted protein, CGP3 region	1.45	**27.59**	n.d.
cg2234		putative ferric dicitrate ABC transporter, secreted substrate-binding lipoprotein	1.68	**6.17**	n.d.
cg2311		putative SAM-dependent methyltransferase	0.91	**5.55**	**2.78**
cg2445	*hmuO*	heme oxygenase	1.85	**5.05**	**4.88**
cg2796		homolog of methylcitrate dehydratase PrpD, MMGE/PRPD family protein	1.06	**18.29**	**2.33**
cg2797		hypothetical protein, conserved	0.78	**5.80**	**4.75**
cg2962		putative heme-degrading monooxygenase	1.49	**12.43**	**6.46**
cg3156	*htaD*	secreted heme transport-associated protein	1.95	**37.26**	n.d.
cg3404		putative ferric dicitrate ABC transporter, secreted substrate-binding lipoprotein	**2.33**	**6.95**	1.24
		RipA regulon			
cg0012	*ssuR*	transcriptional regulator of ROK family	1.25	**3.18**	0.73
cg0310	*katA*	catalase	1.15	**0.05**	**0.48**
cg0445‡	*sdhC*	succinate:menaquinone oxidoreductase, cytochrome *b*	1.45	**0.11**	n.d.
cg0446‡	*sdhA*	succinate:menaquinone oxidoreductase, flavoprotein	1.30	**0.08**	**0.59**
cg0447‡	*sdhB*	succinate:menaquinone oxidoreductase, iron-sulfur protein	1.17	**0.10**	**0.36**
cg0448‡		putative membrane protein	1.14	0.44	1.11
cg1341	*narI*	dissimilatory nitrate reductase, γ-subunit, cytochrome *b*	1.49	**0.07**	n.d.
cg1342	*narJ*	dissimilatory nitrate reductase, δ-subunit, assembly factor	1.51	**0.07**	n.d.
cg1343	*narH*	dissimilatory nitrate reductase, β-subunit, iron-sulfur protein	1.40	**0.11**	**0.32**
cg1344	*narG*	dissimilatory nitrate reductase, α-subunit, Mo cofactor-containing	1.10	**0.07**	**0.24**
cg1345	*narK*	nitrate/nitrite antiporter	1.33	**0.10**	n.d.
cg1487	*leuC*	isopropylmalate isomerase, large subunit	1.24	**0.13**	**0.45**
cg1488	*leuD*	isopropylmalate isomerase, small subunit	0.93	**0.31**	**0.45**
cg1737	*acn*	aconitase	1.30	**0.11**	**0.42**
cg1738	*acnR*	TetR-type transcriptional repressor of *acn* gene	0.95	**0.38**	n.d.
cg2636	*catA*	catechol 1,2-dioxygenase	0.88	**0.05**	**0.39**

Gene locus	Gene name	Annotation	Early: mRNA ratio low/high Fe	Late: mRNA ratio low/high Fe	Late: protein ratio low/high Fe
cg3047	*ackA*	acetate kinase	1.12	**0.13**	**0.44**
cg3048	*pta*	phosphotransacetylase	0.82	**0.10**	**0.45**

[1]Wild-type cells were cultivated in CGXII medium with 222 mM glucose and either low (1 µM $FeSO_4$) or high (36 µM $FeSO_4$) iron levels. The conditions in the pre-cultures were identical to the respective main cultures. Cells were either harvested in the early (OD_{600} 4-5) or late (OD_{600} 12-15) exponential growth phase to extract RNA or protein. Genes with a ≥2-fold altered mRNA ratio either in the early or the late exponential phase and a p value ≤0.05 were used to create the list and mRNA ratios from the other time point were added irrespective of ratio and p value. The protein data were obtained by SWATH-MS analyses using cells in the late exponential growth phase. Mean values from three independent biological replicates are shown. Ratios for which the *p*-value was ≤0.05 are shown in boldface. The complete results of the transcriptome and proteome analyses are shown in Tables S1, S2, and S4. n.d., not detected.

Table 3. Expression of genes subject to control by a TPP riboswitch under iron limitation.

Locus tag	Gene	Annotation	mRNA ratio low/high Fe	p value	protein ratio low/high Fe	p value
cg0825[1]		short chain dehydrogenase	1.37	0.03	1.61	<0.01
cg1227	*ykoE*	ABC transporter for hydroxymethylpyrimidine, permease	3.53	0.02	1.21	0.48
cg1228	*ykoD*	ABC transporter for hydroxymethylpyrimidine, ATPase	3.02	0.01	1.44	<0.01
cg1229	*ykoC*	ABC transporter for hydroxymethylpyrimidine, permease	3.18	0.01	2.97	<0.01
cg1476	*thiC*	phosphomethylpyrimidine synthase	8.41	<0.01	2.47	<0.01
cg1655	*thiM*	hydroxyethylthiazole kinase	1.26	0.27	0.95	0.63
cg2236	*thiE*	thiamin-phosphate pyrophosphorylase	1.81	<0.01	1.53	<0.01
cg2237	*thiO*	putative D-amino acid oxidase flavoprotein oxidoreductase	2.04	0.01	1.25	<0.01
cg2238	*thiS*	sulfur transfer protein involved in thiamine biosynthesis	2.32	<0.01	1.55	0.02
cg2239	*thiG*	thiazole biosynthesis protein	1.90	<0.01	n.d.[2]	
cg2240	*thiF*	dinucleotide-utilizing enzyme involved in thiamine biosynthesis	2.09	<0.01	1.21	0.06

[1]Locus tags with a TPP riboswitch are shown in bold.
[2]n.d., not detected

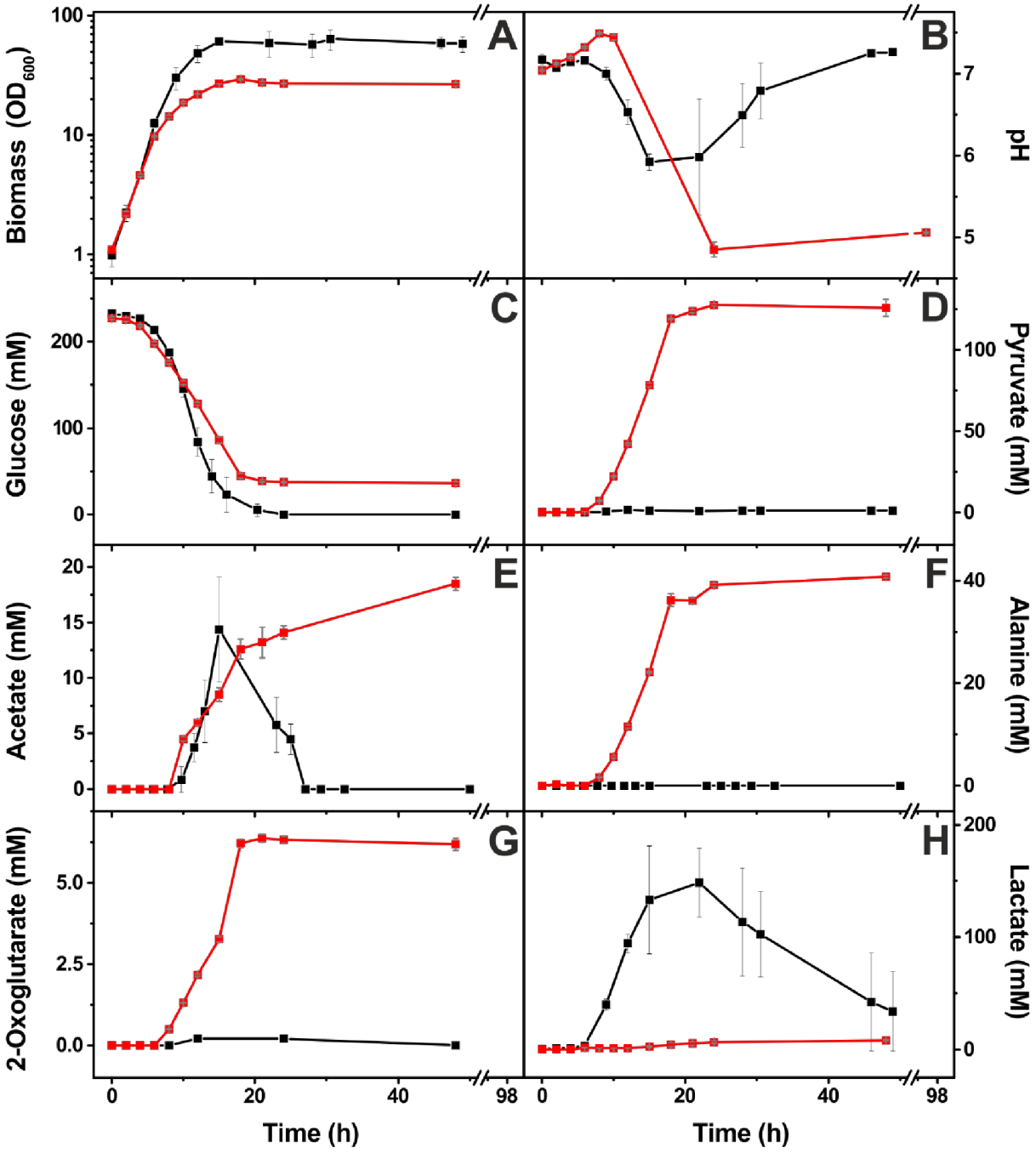

Fig. 1. Influence of different iron concentrations on growth, pH profile, and by-product formation of *C. glutamicum* wild type during cultivation in CGXII minimal medium with 222 mM glucose and either 36 µM $FeSO_4$ (black symbols) or 1 µM $FeSO_4$ (red symbols). Growth was measured as optical density at 600 nm (OD_{600}) (A). Aliquots of the culture supernatants were analyzed with respect to pH (B), glucose consumption (C), and formation of pyruvate (D), acetate (E), L-alanine (F), 2-oxoglutarate (G), and lactate (H). Mean values and standard deviations of three biological replicates are shown. The data of *C. glutamicum* wild type cultivated with 36 µM $FeSO_4$ were taken from a previous study (26).

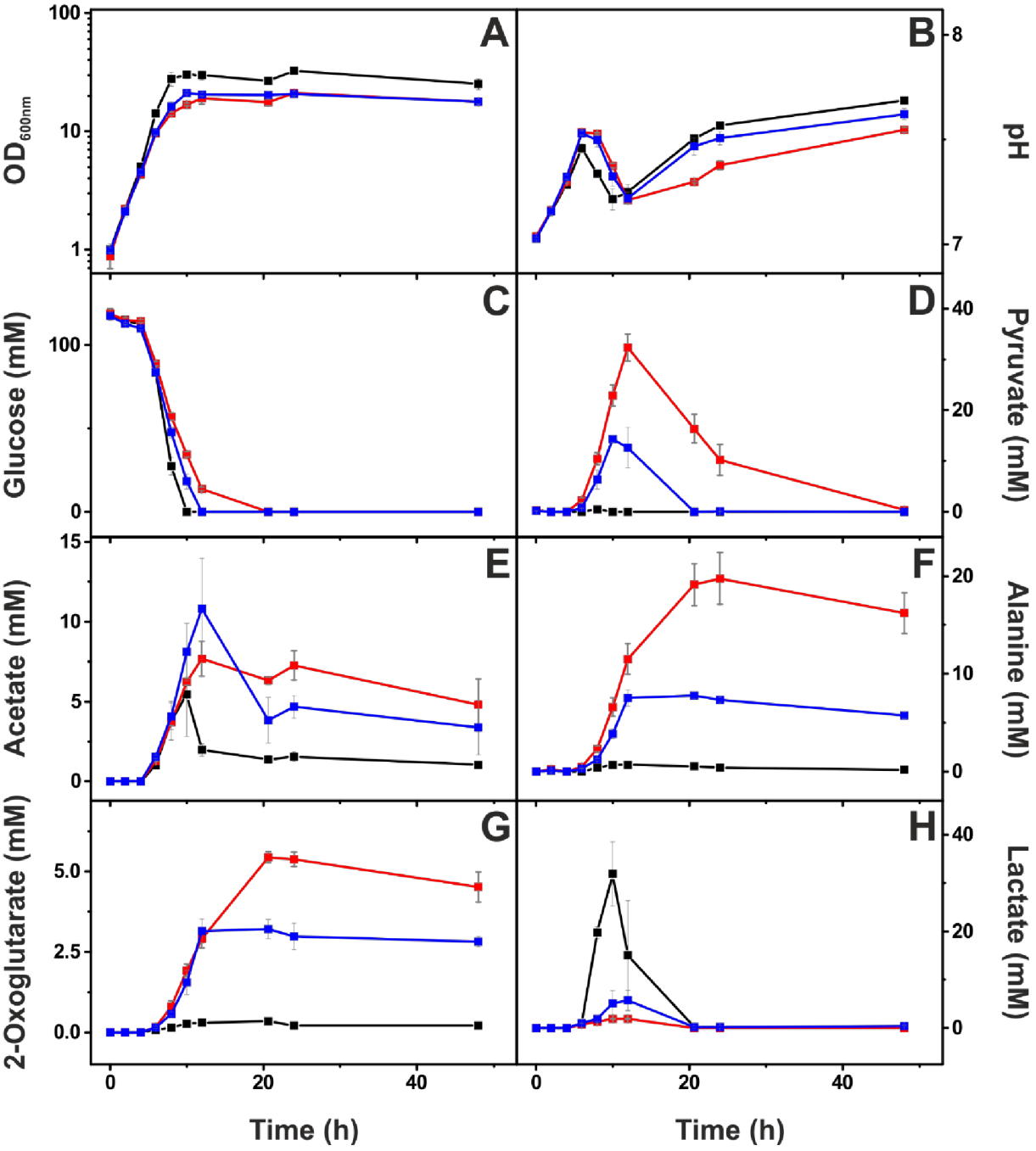

Fig. 2. Influence of different iron concentrations and thiamine on growth, pH profile, and by-product formation of *C. glutamicum* wild type during cultivation in CGXII minimal medium with 111 mM glucose and either 36 µM $FeSO_4$ (black symbols), or 1 µM $FeSO_4$ (red symbols), or 1 µM $FeSO_4$ plus 0.6 µM thiamine (blue symbols). Growth was measured as OD_{600} (A). Aliquots of the culture supernatants were analyzed with respect to pH (B), glucose consumption (C), and formation of pyruvate (D), acetate (E), L-alanine (F), 2-oxoglutarate (G), and lactate (H). Mean values and standard deviations of three biological replicates are shown.

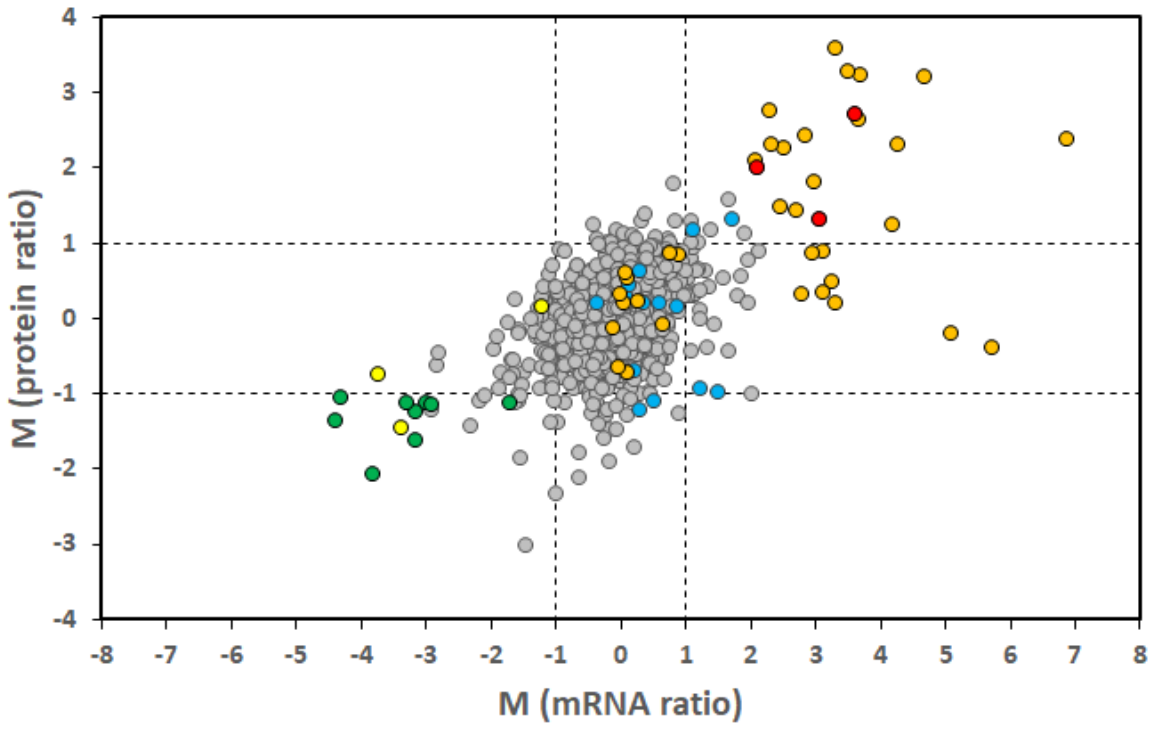

Fig. 3. Correlation of mRNA and protein ratios (1 µM $FeSO_4$ vs. 36 µM $FeSO_4$) in the late exponential growth phase of *C. glutamicum*. Log2 ratios (M values) are plotted for 1116 gene/protein pairs for which both the mRNA ratio and protein ratio could be quantified (●). Members belonging to the DtxR (35 members, ●) and the RipA (9 members, ●) regulon or both (3 members, ●) or to prophage CGP3 (14 members, ●) are highlighted. Genes/proteins *thiC*/ThiC (cg1476), cg2283, and cg2962 showing high ratios are also shown (●). Dashed lines indicate 2-fold ratio change thresholds as Log2.

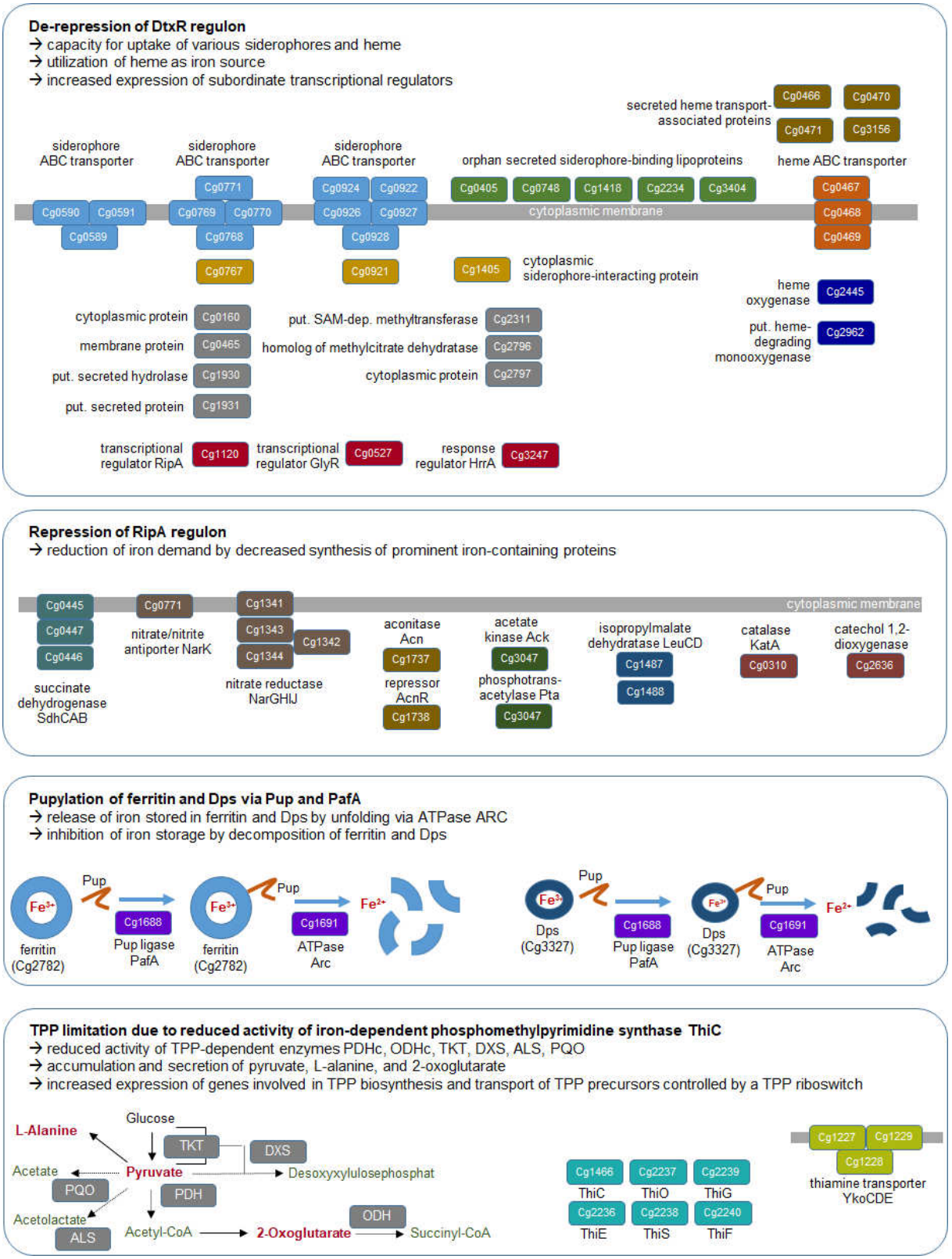

Fig. 4. Schematic overview on iron starvation responses of *C. glutamicum*.

Table S1. Comparison of *C. glutamicum* WT transcriptomes after cultivation under low iron (1 µM $FeSO_4$) and high iron (36 µM) conditions using DNA microarrays. The strains were cultivated in glucose (222 mM) minimal medium; the conditions in precultures were identical to the respective main cultures. Cells were harvested in the early exponential growth phase (OD_{600} 4-5) to extract total RNA. Genes with a ≥2-fold altered average mRNA ratio and a *p*-value ≤0.05 are listed. The values were calculated from three independent biological replicates including one color swap experiment and only genes analyzable in all three experiments were considered. The genes were ordered in functional categories.

Locus tag	Gene Name	Annotation	mRNA ratio low/high Fe	p value
		DtxR regulon		
cg0769		putative siderophore ABC transporter, permease	2.77	0.002
cg0771	*irp1*	putative siderophore ABC transporter, secreted siderophore-binding lipoprotein	2.20	0.004
cg0922		putative secreted siderophore-binding lipoprotein	2.20	0.048
cg3404		putative putative Fe(III) dicitrate ABC transporter, secreted substrate-binding lipoprotein	2.33	0.020
		CGP3 prophage		
cg1895		putative secreted protein, CGP3 region	2.11	0.015
cg1896		putative secreted protein, CGP3 region	4.42	0.011
cg1897		putative secreted protein, CGP3 region	10.97	0.009
cg1914		hypothetical protein, CGP3 region	3.10	0.013
cg1918		putative secreted protein, CGP3 region	6.13	0.021
cg1919		putative membrane protein, CGP3 region	3.41	0.018
cg1922		hypothetical protein, CGP3 region	2.57	0.019
cg1963		putative superfamily II DNA/RNA helicase, CGP3 region	2.20	0.016
cg1970		hypothetical protein, CGP3 region	2.48	0.025
cg1974		putative protein, contains peptidoglycan-binding LysM domain, CGP3 region	3.79	0.023
cg1975		hypothetical protein, conserved, CGP3 region	3.66	0.010
cg1977		putative secreted protein, CGP3 region	5.38	0.003
cg1978		hypothetical protein, CGP3 region	2.02	0.001
cg1980		puative MoxR-like ATPase, CGP3 region	2.00	0.041
cg1983		hypothetical protein, CGP3 region	2.17	0.031
cg1986		hypothetical protein, CGP3 region	2.36	0.026
cg1987		hypothetical protein, CGP3 region	2.09	0.024
cg1999		hypothetical protein, CGP3 region	2.42	0.023
cg2004		puative protein, similar to 232 protein *Lactobacillus* bacteriophage g1e, CGP3 region	2.83	0.021
cg2008		putative membrane protein, CGP3 region	3.16	0.021
cg2014		hypothetical protein, CGP3 region	4.51	0.010
cg2016		hypothetical protein, CGP3 region	3.37	0.010
cg2017		hypothetical protein, CGP3 region	2.79	0.042
cg2061	*psp3*	putative secreted protein, CGP3 region	0.45	0.020
		Transport		
cg0052		putative siderophore ABC transporter, permease	0.49	0.044
cg1377	*ssuC*	aliphatic sulfonates ABC transporter, permease	2.27	0.006
cg1447	*zrf*	zinc exporter, cation diffusion facilitator	2.53	0.021
cg2256		putative multidrug/daunorubicin ABC transporter, ATPase	0.49	0.014
cg3026	*mrpD2*	subunit 3 of Na^+K^+/H^+ antiporter Mrp2	2.08	0.016
cg3226		L-lactate permease	3.25	0.025
cg3353	*nagT*	gentisate transporter	0.50	0.045

		Carbon metabolism		
cg0104	*codA*	creatinine deaminase	0.48	0.003
cg0341	*phdA*	acyl:CoA ligase transmembrane protein; involved in degradation of aromatic compounds	0.43	0.009
cg1320	*lipP*	lipase, conserved	0.45	0.033
cg2637	*benA*	benzoate 1,2-dioxygenase	0.44	0.012
		Further genes		
cg0079		putative secreted protein	0.47	0.043
cg0255		hypothetical protein	0.45	0.024
cg0713		hypothetical protein, conserved	2.19	0.036
cg1279		putative secreted protein	2.26	0.035
cg1369	*atpC*	F_1F_O-ATP synthase, ε-subunit of F_1 part	2.05	0.045
cg1513	*tnp23a*	transposase, putative pseudogene, CGP1 region	2.90	0.006
cg2511		putative membrane protein containing CBS domain	2.35	0.007
cg2756		hypothetical protein, conserved	0.43	0.000
cg2804	*tnp21a*	transposase	0.45	0.034
cg3103		hypothetical protein, conserved	0.32	0.014
cg3297	*tnp19b*	transposase fragment, putative pseudogene	0.50	0.040
cg4005		putative secreted protein, CGP1 region	2.48	0.047

Table S2. Comparison of *C. glutamicum* WT transcriptomes after cultivation under low iron (1 µM $FeSO_4$) and high iron (36 µM) conditions using DNA microarrays. The strains were cultivated in glucose (222 mM) minimal medium; the conditions in precultures were identical to the respective main cultures. Cells were harvested in the late exponential growth phase (OD_{600} 12–15) to extract total RNA. Genes with a ≥2-fold altered average mRNA ratio and a *p*-value ≤0.05 are listed. The values were calculated from three independent biological replicates including one color swap experiment and only genes analyzable in all three experiments were considered. Genes labeled with asterisk are regulated both by DtxR and RipA. Genes colored in orange were ≥5-fold upregulated under iron deprivation, genes colored in green were ≥5-fold downregulated under iron deprivation. In the right two columns the results of a proteome comparison of cells grown under the same conditions as described above are listed. The relative protein ratios and *p*-values were calculated from three biological replicates with two technical replicates for each biological replicate, i.e. from six measurements each for cells grown under low and high iron conditions. n.d., not detectable.

Gene locus	Gene name	Annotation	mRNA ratio low/high Fe	*p* value	Protein ratio low/high Fe	*p* value
		DtxR regulon				
cg0160		hypothetical protein	10.95	0.002	n.d.	
cg0405		putative ferric dicitrate ABC transporter, secreted siderophore-binding lipoprotein	10.05	0.005	11.95	0.001
cg0465		putative membrane protein, conserved	10.22	0.009	n.d.	
cg0466	*htaA*	secreted heme transport-associated protein	11.93	0.003	n.d.	
cg0467	*hmuT*	heme ABC transporter, secreted heme-binding lipoprotein	8.83	0.003	1.82	0.018
cg0468	*hmuU*	heme ABC transporter, permease	7.28	0.002	n.d.	
cg0469	*hmuV*	heme ABC transporter, ATPase	4.27	0.023	n.d.	
cg0470	*htaB*	secreted heme transport-associated protein	118.62	0.011	5.17	0.001
cg0471	*htaC*	secreted heme transport-associated protein	53.40	0.014	0.75	0.525
cg0527	*glyR*	ArsR-type transcriptional regulator of *glyA*	7.89	0.028	1.80	0.238
cg0589		putative siderophore ABC transporter, ATPase	9.69	0.003	1.39	0.034
cg0590		putative siderophore ABC transporter, permease	11.39	0.002	9.58	0.001
cg0591		putative siderophore ABC transporter, permease	5.94	0.001	n.d.	
cg0748		putative siderophore ABC transporter, substrate-binding lipoprotein	4.93	0.007	6.70	0.001
cg0767		putative cytoplasmic siderophore-interacting protein	7.25	0.004	5.36	0.001
cg0768		putative siderophore ABC transporter, ATPase	10.01	0.004	1.14	0.378
cg0769		putative siderophore ABC transporter, permease	6.87	0.002	n.d.	
cg0770		putative siderophore ABC transporter, permease	10.28	0.008	n.d.	

cg0771	*irp1*	putative siderophore ABC transporter, secreted siderophore-binding lipoprotein	12.77	0.005	6.18	0.001
cg0921		putative cytoplasmic siderophore-interacting protein	14.81	0.006	n.d.	
cg0922		putative secreted siderophore-binding lipoprotein	19.62	0.002	4.87	0.001
cg0924		putative siderophore ABC transporter, secreted substrate-binding lipoprotein	12.97	0.004	9.29	0.001
cg0926		putative siderophore ABC transporter, permease	6.42	0.002	n.d.	
cg0927		putative siderophore ABC transporter, permease	8.81	0.001	1.25	0.102
cg0928		putative siderophore ABC transporter, ATPase	4.30	0.025	4.23	0.001
cg1120	*ripA*	transcriptional regulator of iron proteins and repressor of aconitase, AraC-family	25.83	0.006	9.14	0.001
cg1405		putative cytoplasmic siderophore-interacting protein	6.63	0.002	2.69	0.001
cg1418		putative secreted siderophore-binding lipoprotein	7.94	0.001	3.49	0.001
cg1930		putative secreted hydrolase, CGP3 region	34.35	0.004	0.86	0.843
cg1931		putative secreted protein, CGP3 region	27.59	0.003	n.d.	
cg2234		putative iron(III) dicitrate ABC transporter, secreted substrate-binding lipoprotein	6.17	0.006	n.d.	
cg2311		putative SAM-dependent methyltransferase	5.55	0.003	2.78	0.001
cg2445	*hmuO*	heme oxygenase	5.05	0.006	4.88	0.001
cg2796		homolog of methylcitrate dehydratase PrpD, MMGE/PRPD-family protein	18.29	0.002	2.33	0.001
cg2797		hypothetical protein, conserved	5.80	0.012	4.75	0.001
cg3156	*htaD*	secreted heme transport-associated protein	37.26	0.007	n.d.	
cg3404		putative iron(III) dicitrate ABC transporter, substrate-binding lipoprotein	6.95	0.005	1.24	0.255
		RipA regulon				
cg0310	*katA*	catalase	0.05	0.001	0.48	0.001
cg0445*	*sdhC*	succinate:menaquinone oxidoreductase, cytochrome *b* subunit	0.11	0.001	n.d.	
cg0446*	*sdhA*	succinate:menaquinone oxidoreductase, flavoprotein subunit	0.08	0.001	0.59	0.003
cg0447*	*sdhB*	succinate:menaquinone oxidoreductase, iron-sulfur protein subunit	0.10	0.001	0.36	0.046
cg0448*		putative membrane protein	0.44	0.040	1.11	0.636

cg1341	*narI*	dissimilatory nitrate reductase, γ-subunit, cytochrome *b*	0.07	0.002	n.d.	
cg1342	*narJ*	dissimilatory nitrate reductase, δ-subunit, assembly factor	0.07	0.003	n.d.	
cg1343	*narH*	dissimilatory nitrate reductase, β-subunit, iron sulfur protein	0.11	0.002	0.32	0.027
cg1344	*narG*	dissimilatory nitrate reductase, α-subunit, Mo cofactor-containing	0.07	0.004	0.24	0.007
cg1345	*narK*	nitrate/nitrite antiporter	0.10	0.004	n.d.	
cg1487	*leuC*	isopropylmalate isomerase, large subunit	0.13	0.003	0.45	0.011
cg1488	*leuD*	isopropylmalate isomerase small subunit	0.31	0.035	0.45	0.005
cg1737	*acn*	aconitase	0.11	0.001	0.42	0.001
cg1738	*acnR*	transcriptional regulator of TetR family, represses *acn*	0.38	0.012	n.d.	
cg2636	*catA*	catechol 1,2-dioxygenase	0.05	0.001	0.39	0.002
cg3047	*ackA*	acetate kinase	0.13	0.005	0.44	0.001
cg3048	*pta*	phosphotransacetylase	0.10	0.001	0.45	0.001
		CGP3 prophage				
cg1896		putative secreted protein, CGP3 region	3.06	0.005	n.d.	
cg1897		putative secreted protein, CGP3 region	3.83	0.001	n.d.	
cg1918		putative secreted protein, CGP3 region	4.62	0.012	n.d.	
cg1919		putative membrane protein, CGP3 region	2.01	0.016	n.d.	
cg1940		putative secreted protein, CGP3 region	2.88	0.039	n.d.	
cg1941		putative secreted protein, CGP3 region	2.34	0.001	n.d.	
cg1957		hypothetical protein, CGP3 region	2.46	0.016	n.d.	
cg1968		hypothetical protein, CGP3 region	2.28	0.010	n.d.	
cg1974		putative protein, contains peptidoglycan-binding LysM domain, CGP3 region	2.75	0.009	n.d.	
cg1975		hypothetical protein, conserved, CGP3 region	2.33	0.020	n.d.	
cg1977		putative secreted protein, CGP3 region	3.33	0.006	2.45	0.001
cg1978		hypothetical protein, CGP3 region	2.04	0.001	n.d.	
cg1994		hypothetical protein, CGP3 region	2.04	0.010	n.d.	
cg1999		hypothetical protein, CGP3 region	2.18	0.010	n.d.	
cg2004		putative protein, similar to 232 protein of *Lactobacillus* bacteriophage g1e, conserved, CGP3 region	2.38	0.003	n.d.	
cg2008		putative membrane protein, CGP3 region	2.39	0.001	n.d.	
cg2009		putative CLP-family ATP-binding protease, CGP3 region	2.09	0.027	n.d.	

cg2011		putative membrane protein, CGP3 region	2.36	0.038	n.d.	
cg2014		hypothetical protein, CGP3 region	3.54	0.001	n.d.	
cg2015		hypothetical protein, CGP3 region	2.27	0.008	n.d.	
cg2016		hypothetical protein, CGP3 region	2.83	0.019	n.d.	
cg2017		hypothetical protein, CGP3 region	2.86	0.001	0.50	0.198
cg2018		putative membrane protein, CGP3 region	3.15	0.007	n.d.	
cg2019		putative membrane protein, CGP3 region	2.02	0.034	n.d.	
cg2022		putative secreted protein, CGP3 region	2.47	0.007	n.d.	
cg2023		putative membrane protein, CGP3 region	2.08	0.003	n.d.	
cg2032		putative membrane protein, CGP3 region	2.01	0.010	n.d.	
cg2046		hypothetical protein, CGP3 region	2.02	0.040	n.d.	
cg2052		putative secreted protein, CGP3 region	2.19	0.040	2.24	0.001
cg2062		putative protein, similar to plasmid-encoded protein PXO2.09, CGP3 region	2.20	0.026	n.d.	
cg2063		putative membrane protein, CGP3 region	2.33	0.017	n.d.	
cg2064		putative DNA topoisomerase ω protein, CGP3 region	2.36	0.042	0.52	0.300
		Transport				
cg0083		putative nicotinamide mononucleotide uptake permease, PnuC-family	2.47	0.009	n.d.	
cg0133	*abgT*	*p*-aminobenzoyl-glutamate transporter	0.30	0.003	n.d.	
cg0506		ABC transporter for spermidine or putrescine or iron(III), ATPase subunit	0.26	0.024	n.d.	
cg0507		ABC transporter for spermidine or putrescine or iron(III), permease	0.19	0.003	n.d.	
cg0508		ABC transporter for spermidine or putrescine or iron(III), secreted substrate-binding lipoprotein	0.18	0.001	n.d.	
cg0701		putative drug/metabolite transporter, DMT superfamily	2.11	0.009	n.d.	
cg0737	*metQ*	ABC transporter for methionine, secreted substrate-binding lipoprotein	2.14	0.019	1.72	0.001
cg0831	*tusG*	trehalose ABC transporter, permease	0.49	0.019	n.d.	
cg0832	*tusF*	trehalose ABC-transporter, permease	0.35	0.009	n.d.	
cg0833		putative membrane protein, involved in trehalose uptake, conserved	0.31	0.004	n.d.	
cg0834	*tusE*	trehalose ABC transporter, secreted solute-binding lipoprotein	0.38	0.001	n.d.	
cg0953	*mctC*	monocarboxylic acid transporter	0.48	0.022	0.70	0.269

cg1088		putative multidrug/protein/lipid ABC transporter, ATPase	2.10	0.008	n.d.	
cg1109	*porB*	anion-specific porin precursor	0.47	0.016	1.48	0.070
cg1121		putative permease of the major facilitator superfamily	2.66	0.016	n.d.	
cg1169	*metP*	secondary methionine uptake system of the neurotransmitter:sodium symporter family	0.47	0.006	0.64	0.119
cg1227	*ykoE*	putative thiamin-regulated ABC transporter for hydroxymethyl-pyrimidine, permease	3.53	0.002	1.21	0.483
cg1228	*ykoD*	putative thiamin-regulated ABC transporter for hydroxymethyl-pyrimidine, duplicated ATPase component	3.02	0.012	1.44	0.001
cg1229	*ykoC*	putative thiamin-regulated ABC transporter for hydroxymethyl-pyrimidine, permease	3.18	0.011	2.97	0.001
cg1231	*chaA*	$Na^+(K^+)/H^+$ antiporter	2.91	0.001	n.d.	
cg1419		putative Na^+-dependent transporter, bile acid:Na^+ symporter BASS-family	4.96	0.001	n.d.	
cg1785	*amtA*	high-affinity ammonia permease	2.07	0.007	n.d.	
cg2136	*gluA*	glutamate ABC transporter, ATPase	0.44	0.007	1.19	0.277
cg2137	*gluB*	glutamate ABC transporter, secreted glutamate-binding lipoprotein	0.47	0.010	0.92	0.375
cg2138	*gluC*	glutamate ABC transporter, permease	0.45	0.006	1.32	0.191
cg2139	*gluD*	glutamate ABC transporter, permease	0.50	0.030	n.d.	
cg2181	*oppA*	peptide ABC transporter, secreted lipoprotein	0.26	0.006	0.75	0.011
cg2182	*oppB*	peptide ABC transporter, permease	0.28	0.009	n.d.	
cg2468		putative branched-chain amino acid ABC transporter, permease	0.50	0.034	n.d.	
cg2470		putative branched-chain amino acid ABC transporter, secreted substrate-binding lipoprotein	0.44	0.022	1.01	0.927
cg2557		putative secondary Na^+/bile acid symporter, BASS family	0.36	0.001	n.d.	
cg2610		putative dipeptide/oligopeptide/nickel ABC transporter, secreted lipoprotein	0.19	0.002	n.d.	
cg2675		putative dipeptide ABC transporter, duplicated ATPase domains	4.11	0.017	0.49	0.036
cg2676		putative dipeptide ABC transporter, permease	4.14	0.003	n.d.	
cg2677		putative dipeptide ABC transporter, permease	4.40	0.001	1.83	0.008
cg2678		putative dipeptide ABC transporter, secreted substrate-binding lipoprotein	3.92	0.003	1.68	0.001
cg2884		putative dipeptide/tripeptide permease	0.42	0.005	n.d.	

cg2937	*siaE*	sialic acid ABC transporter, secreted component	0.39	0.030	0.99	0.813
cg2939	*siaG*	sialic acid ABC transporter, fused permease and ATPase	0.44	0.027	n.d.	
cg3126	*tctB*	tripartite citrate transporter, membrane subunit	0.45	0.024	n.d.	
cg3130		putative permease of the major facilitator superfamily	0.40	0.036	n.d.	
cg3216	*gntP*	gluconate permease	0.27	0.005	n.d.	
cg3226		L-lactate permease	0.29	0.013	n.d.	
cg3295		putative Cd^{2+}/cation transport ATPase	2.10	0.026	n.d.	
cg3399		putative permease of the major facilitator superfamily	2.33	0.009	n.d.	
cg3403		putative permease of the major facilitator superfamily	2.18	0.046	n.d.	
		Respiration				
cg1300	*cydB*	cytochrome *bd* oxidase, subunit II	0.35	0.031	n.d.	
cg2403	*qcrB*	cytochrome bc_1 complex, cytochrome *b* subunit	0.34	0.005	0.49	0.011
cg2404	*qcrA*	cytochrome bc_1 complex, Rieske iron-sulfur protein	0.28	0.003	0.52	0.014
cg2405	*qcrC*	cytochrome bc_1 complex, diheme cytochrome c_1	0.27	0.002	0.83	0.262
cg2406	*ctaE*	cytochrome aa_3 oxidase, subunit 3	0.30	0.006	n.d.	
cg2408	*ctaF*	cytochrome aa_3 oxidase, subunit 4	0.49	0.046	n.d.	
cg2409	*ctaC*	cytochrome aa_3 oxidase, subunit 2	0.46	0.019	n.d.	
cg2780	*ctaD*	cytochrome aa_3 oxidase, subunit 1	0.47	0.009	0.71	0.072
cg2891	*pqo*	pyruvate:quinone oxidoreductase	2.05	0.003	1.52	0.001
		Carbon metabolism				
cg0387	*adhE*	mycothiol-dependent formaldehyde dehydrogenase	2.07	0.022	1.82	0.001
cg0592		putative butyryl-CoA:acetate coenzyme A transferase	2.26	0.019	n.d.	
cg0638	*creD*	*p*-cresol methylhydroxylase subunit	0.44	0.009	n.d.	
cg0639	*creE*	ferredoxin reductase, part of putative cytochrome P450 system of *p*-cresol methylhydroxylase	0.40	0.006	n.d.	
cg0644	*creI*	4-methylbenzyl phosphate synthase	0.38	0.050	n.d.	
cg0645	*creJ*	component of class I P450 system oxidizing the methyl group of phosphorylated *p*-cresol	0.25	0.013	n.d.	
cg0759	*prpD2*	2-methycitrate dehydratase	0.14	0.013	0.64	0.002
cg0760	*prpB2*	2-methylisocitrate lyase	0.13	0.011	0.43	0.085
cg0762	*prpC2*	2-methylcitrate synthase	0.11	0.016	n.d.	
cg1724	*meaB*	accessory protein of methylmalonyl-CoA mutase	0.32	0.003	0.67	0.001
cg1725	*mcmB*	methylmalonyl-CoA mutase, α subunit	0.32	0.012	0.59	0.002

cg1726	*mcmA*	methylmalonyl-CoA mutase, β subunit	0.22	0.010	0.46	0.010
cg1853	*glpD*	glycerol-3-phosphate dehydrogenase	0.44	0.012	1.22	0.322
cg2284	*galT*	galactose-1-phosphate uridylyltransferase	0.33	0.005	n.d.	
cg2559	*aceB*	malate synthase	2.63	0.005	2.24	0.001
cg2560	*aceA*	isocitrate lyase	2.30	0.008	1.97	0.001
cg2616	*vanA*	vanillate demethylase, oxygenase subunit	0.42	0.005	n.d.	
cg2630	*pcaG*	protocatechuate dioxygenase, α subunit	0.35	0.007	0.53	0.241
cg2631	*pcaH*	protocatechuate dioxygenase, β subunit	0.33	0.006	0.46	0.001
cg2836	*sucD*	succinyl-CoA synthetase, α subunit	0.35	0.006	0.27	0.013
cg2837	*sucC*	succinyl-CoA synthetase, β subunit	0.35	0.023	0.49	0.001
cg2958	*butA*	L-2,3-butanediol dehydrogenase/acetoin reductase	2.38	0.021	1.29	0.047
cg2966		putative phenol 2-monooxygenase	0.31	0.015	n.d.	
cg3107	*adhA*	Zn-dependent alcohol dehydrogenase	0.42	0.001	1.00	0.954
cg3158	*nagA2*	β-N-acetylglucosaminidase	0.46	0.004	n.d.	
cg3198	*glpK*	glycerol kinase	0.30	0.005	0.95	0.623
cg3212		putative carboxymuconolactone decarboxylase subunit	0.47	0.015	n.d.	
cg3386	*tcbF*	maleylacetate reductase	0.49	0.009	0.51	0.158
		Cofactor biosynthesis				
cg0095	*bioB*	biotin synthase	0.34	0.007	0.46	0.011
cg0148	*panC*	pantoate-β-alanine ligase protein	0.48	0.006	0.62	0.034
cg0172	*panD*	aspartate 1-decarboxylase	0.27	0.003	n.d.	
cg1352	*moaA*	molybdenum cofactor biosynthesis protein A	2.84	0.001	n.d.	
cg1476	*thiC*	phosphomethylpyrimidine synthase involved in thiamine biosynthesis	8.41	0.001	2.47	0.001
cg2237	*thiO*	putative D-amino acid oxidase, flavoprotein oxidoreductase	2.04	0.013	1.25	0.001
cg2238	*thiS*	sulfur transfer protein involved in thiamine biosynthesis	2.32	0.001	1.55	0.017
cg2240	*thiF*	molybdopterin biosynthesis protein MoeB, involved in thiamine biosynthesis	2.09	0.004	1.21	0.063
cg2422	*lipB*	lipoyltransferase	0.31	0.014	0.57	0.078
		Regulation				
cg0012	*ssuR*	sulphonate sulphur utilization transcriptional regulator SsuR, activator of sulfonate ester utilization, ROK-family	3.18	0.004	0.73	0.299
cg0228	*hkm*	putative histidine kinase fragment of two-component system, putative pseudogene	0.15	0.004	n.d.	

cg1456		putative signal-transduction protein containing cAMP-binding and CBS domain, conserved	0.44	0.003	0.85	0.169
cg2761	*cpdA*	cAMP phosphodiesterase	0.48	0.001	0.38	0.113
cg2965		AraC-type transcriptional regulator	0.42	0.024	n.d.	
cg3303		PadR-family transcriptional regulator	0.28	0.001	n.d.	
cg3388		IclR-type transcriptional regulator	0.45	0.002	n.d.	
		Amino acid biosynthesis				
cg0755	*metY*	O-acetylhomoserine sulfhydrylase	2.51	0.010	1.52	0.001
cg1290	*metE*	5-methyltetrahydropteroyl-triglutamate-homocysteine methyltransferase	0.48	0.001	0.60	0.001
cg1432	*ilvD*	dihydroxy-acid dehydratase	0.32	0.018	0.67	0.001
cg1435	*ilvB*	acetolactate synthase, large subunit	0.40	0.006	0.87	0.001
cg1436	*ilvN*	acetolactate synthase, small subunit	0.33	0.004	1.18	0.285
cg2779	*serB*	phosphoserine phosphatase	0.24	0.010	0.49	0.001
cg2833	*cysK*	O-acetylserine (thiol)-lyase, cysteine synthase	2.14	0.006	1.99	0.001
		Translation				
cg0526		putative translation initiation inhibitor, YjgF family, PFAM domain endoribonuclease L-PSP	2.22	0.042	n.d.	
cg0563	*rplK*	50S ribosomal protein L11	0.47	0.003	1.13	0.212
cg0594	*rplC*	50S ribosomal protein L3	0.45	0.015	0.53	0.071
cg0598	*rplB*	50S ribosomal protein L2	0.43	0.001	0.83	0.104
cg0599	*rpsS*	30S ribosomal protein S19	0.46	0.004	0.63	0.049
cg0989	*rpsN*	30S ribosomal protein S14	0.48	0.007	0.65	0.226
cg1333	*argS*	arginyl-tRNA synthetase	0.45	0.001	1.17	0.419
cg2135	*miaB*	tRNA methylthiotransferase	0.23	0.003	n.d.	
cg2594	*rpmA*	50S ribosomal protein L27	0.50	0.023	0.46	0.077
		Further genes				
cg0096		hypothetical protein, conserved	0.34	0.001	0.90	0.784
cg0097		putative zinc finger protein, conserved	0.35	0.008	n.d.	
cg0134	*abgB*	putative zinc metallopeptidase	0.41	0.017	0.83	0.099
cg0175		putative secreted protein	2.08	0.013	n.d.	
cg0177		hypothetical protein	8.16	0.001	n.d.	
cg0316		putative secreted protein	2.37	0.006	n.d.	
cg0404		putative protein of nitroreductase family, conserved	2.16	0.013	1.28	0.078
cg0493		hypothetical protein	0.49	0.006	n.d.	
cg0704		conserved protein of unknown function, PFAM Imm68	2.15	0.001	2.41	0.001
cg0712		putative secreted protein	0.23	0.001	n.d.	
cg0726		putative secreted lipoprotein	2.26	0.006	n.d.	

cg0752		putative secreted or membrane protein	2.21	0.009	1.22	0.222
cg0810	*accE*	ε-subunit of acetyl-CoA carboxylase	0.50	0.027	1.00	0.967
cg0845		putative superfamily II DNA/RNA helicase, SNF2-family	0.46	0.005	0.70	0.005
cg0951	*accD3*	acetyl-coenzyme A carboxylase, carboxyl transferase	0.44	0.009	0.73	0.059
cg0961		protein of alpha/beta hydrolase superfamily	0.42	0.010	1.08	0.829
cg1090	*ggtB*	probable γ-glutamyltranspeptidase	0.34	0.006	0.86	0.521
cg1091		hypothetical protein	2.55	0.017	n.d.	
cg1147	*ssuI*	NADPH-dependent FMN reductase	2.23	0.002	n.d.	
cg1150		putative NADPH-dependent FMN reductase	2.20	0.017	1.90	0.012
cg1206		putative PEP phosphonomutase or related enzyme, conserved	2.24	0.011	1.24	0.053
cg1230		hypothetical protein, conserved	2.48	0.014	n.d.	
cg1236	*tpx*	thiol peroxidase	2.16	0.041	0.73	0.217
cg1304		putative secreted protein	0.49	0.044	n.d.	
cg1307		putative superfamily II DNA and RNA helicase	2.39	0.006	1.06	0.047
cg1312		putative membrane protein	0.36	0.006	n.d.	
cg1373		putative glyoxalase/bleomycin resistance/dioxygenase superfamily protein	0.28	0.004	0.60	0.034
cg1457	*dnaQ2*	putative DNA polymerase III, ε subunit	0.39	0.009	n.d.	
cg1475		hypothetical protein, conserved	2.15	0.003	n.d.	
cg1490		putative NTP pyrophosphohydrolase including oxidative damage repair enzyme	0.36	0.010	0.60	0.058
cg1513	*tnp23a*	transposase, putative pseudogene, CGP1 region	3.26	0.018	n.d.	
cg1514		putative secreted protein, CGP1 region	3.80	0.001	2.17	0.022
cg1612		putative acetyltransferase	0.20	0.009	0.37	0.032
cg1626		conserved protein of unkown function	5.52	0.011	n.d.	
cg1628		putative hydrolase of the α/β superfamily	4.20	0.045	n.d.	
cg1694	*recB*	RecB-family exonuclease	0.16	0.002	n.d.	
cg1695		putative plasmid maintenance system antidote protein, HTH-motif XRE-family	0.19	0.014	n.d.	
cg1736		putative membrane protein	0.30	0.044	n.d.	
cg1740		putative nucleoside diphosphate sugar epimerase	2.74	0.005	0.93	0.790
cg1883		putative secreted protein	0.45	0.002	0.71	0.022
cg2211		putative membrane protein	0.43	0.002	0.51	0.071
cg2252		putative double-stranded β-helix domain	2.60	0.016	1.31	0.147
cg2283		hypothetical protein	4.38	0.004	3.96	0.001

cg2411		putative protein of HesB/YadR/YfhF-family, conserved	2.09	0.012	1.44	0.001
cg2438		hypothetical protein	0.46	0.024	n.d.	
cg2444		hypothetical protein	2.29	0.013	1.54	0.105
cg2556		putative iron-regulated membrane protein	0.36	0.004	n.d.	
cg2674		putative alkylhydroperoxidase, AhpD family core domain	2.38	0.003	0.98	0.941
cg2777		putative membrane protein, conserved	2.49	0.001	n.d.	
cg2778		hypothetical protein, conserved	0.22	0.003	n.d.	
cg2828		putative membrane protein	0.47	0.025	n.d.	
cg2861		putative membrane protein, hemolysin III homolog	0.44	0.004	n.d.	
cg2890		putative amino acid processing enzyme	2.19	0.001	n.d.	
cg2949		putative secreted protein	0.49	0.009	n.d.	
cg2954	*cynT*	carbonic anhydrase	0.44	0.005	0.63	0.001
cg2962		putative heme-degrading monooxygenase	12.43	0.005	6.46	0.001
cg3073	*sseA1*	putative thiosulfate sulfurtransferase protein	2.61	0.011	n.d.	
cg3136		putative nitroreductase	2.13	0.024	n.d.	
cg3141	*hmp*	flavohemoprotein	4.21	0.011	n.d.	
cg3190		putative membrane-associated phospholipid phosphatase	0.49	0.002	1.61	0.069
cg3191	*glfT*	putative glycosyltransferase	0.49	0.002	0.54	0.033
cg3195		putative flavin-containing monooxygenase	0.14	0.008	0.72	0.033
cg3260		putative membrane protein	0.49	0.034	n.d.	
cg3267		putative membrane protein, putative pseudogene, C-terminal fragment	2.21	0.004	n.d.	
cg3274		putative site-specific recombinase, putative pseudogene	2.34	0.034	n.d.	
cg3292		putative copper chaperone	3.03	0.014	n.d.	
cg3341		putative membrane protein	0.42	0.007	n.d.	
cg3369	*qcrA2*	iron-sulfur protein of unknown function	0.42	0.013	n.d.	
cg3372		hypothetical protein, conserved	3.66	0.007	1.46	0.250
cg3396		putative membrane protease subunit, stomatin/prohibitin homologs	2.55	0.017	0.76	0.471
cg3431	*rnpA*	ribonuclease P	0.47	0.003	0.62	0.127
cg4005		putative secreted protein, CGP1 region	3.94	0.017	1.14	0.740

Table S5. Functional categorization of *C. glutamicum* WT proteins with at least two-fold altered levels under iron deficiency. The cells were cultivated in glucose (222 mM) minimal medium with either 36 µM $FeSO_4$ or 1 µM $FeSO_4$. The conditions in precultures were identical to the respective main cultures. Cells were harvested in the late (OD_{600} 12–15) exponential growth phase to extract total protein. Proteins with a ≥2-fold altered average protein ratio and a *p*-value ≤0.05 are listed. The protein ratios and *p*-values were calculated by SWATH-MS from three biological replicates with two technical replicates for each biological replicate, i.e. from six measurements each for cells grown under low and high iron conditions (see Table S4). In the right two columns the results of a transcriptome comparison of cells grown under the same conditions as described above are listed. The transcriptome values are also based on three biological replicates.

Locus tag	Gene	Annotation	Protein ratio low/high Fe	p value	mRNA ratio low/high Fe	p value
		DtxR regulon				
cg0405		putative ferric dicitrate ABC transporter, secreted siderophore-binding lipoprotein	11.95	0.001	10.05	0.005
cg0470	*htaB*	secreted heme transport-associated protein	5.17	0.001	118.62	0.011
cg0590		putative siderophore ABC transporter, permease protein	9.58	0.001	11.39	0.002
cg0748		putative ABC-type putative iron-siderophore transporter, substrate-binding lipoprotein	6.70	0.001	4.93	0.007
cg0767		putative cytoplasmic siderophore-interacting protein	5.36	0.001	7.25	0.004
cg0771	*irp1*	putative iron-siderophore ABC transporter, secreted siderophore-binding lipoprotein	6.18	0.001	12.77	0.005
cg0922		putative secreted siderophore-binding lipoprotein	4.87	0.001	19.62	0.002
cg0924		putative ABC-type putative iron-siderophore transporter, substrate-binding lipoprotein	9.29	0.001	12.97	0.004
cg0928		putative ABC-type putative iron-siderophore transporter, ATPase subunit	4.23	0.001	4.30	0.025
cg1120	*ripA*	transcriptional regulator of iron proteins and repressor of aconitase, AraC-family	9.14	0.001	25.83	0.006
cg1405		putative cytoplasmic siderophore-interacting protein	2.69	0.001	6.63	0.002
cg1418		putative secreted siderophore-binding lipoprotein	3.49	0.001	7.94	0.001
cg2311		putative SAM-dependent methyltransferase	2.78	0.001	5.55	0.003
cg2445	*hmuO*	heme oxygenase	4.88	0.001	5.05	0.006
cg2796		putative MMGE/PRPD-family protein, putative involved in propoinate catabolism, conserved	2.33	0.001	18.29	0.002
cg2797		hypothetical protein, conserved	4.75	0.001	5.80	0.012
		RipA regulon				
cg0310	*katA*	catalase	0.48	0.001	0.05	0.001

cg0447	*sdhB*	succinate:menaquinone oxidoreductase, iron-sulfur protein	0.36	0.046	0.10	0.001
cg1343	*narH*	dissimilatory nitrate reductase, β-subunit, iron sulfur protein	0.32	0.027	0.11	0.002
cg1344	*narG*	dissimilatory nitrate reductase, α-subunit, Mo cofactor-containing protein	0.24	0.007	0.07	0.004
cg1487	*leuC*	isopropylmalate isomerase, large subunit	0.45	0.011	0.13	0.003
cg1488	*leuD*	isopropylmalate isomerase, small subunit	0.45	0.005	0.31	0.035
cg1737	*acn*	aconitase	0.42	0.001	0.11	0.001
cg2636	*catA*	catechol 1,2-dioxygenase	0.39	0.002	0.05	0.001
cg3047	*ackA*	acetate kinase	0.44	0.001	0.13	0.005
cg3048	*pta*	phosphotransacetylase	0.45	0.001	0.10	0.001
		CGP3 prophage				
cg1977		putative secreted protein CGP3 region	2.45	0.001	3.33	0.006
cg2052		putative secreted protein CGP3 region	2.24	0.001	2.19	0.040
		Transport				
cg1229	*ykoC*	putative thiamin-regulated ABC transporter for hydroxymethylpyrimidine, permease	2.97	0.001	3.18	0.011
cg2675		putative dipeptide ABC transporter, duplicated ATPase domains	0.49	0.036	4.11	0.017
		Respiration				
cg3405		putative NADPH quinone reductase or Zn-dependent oxidoreductase	2.44	0.002	1.80	0.014
cg2403	*qcrB*	cytochrome bc_1 complex, cytochrome *b* subunit	0.49	0.011	0.34	0.005
		Carbon metabolism				
cg0457	*purU*	formyltetrahydrofolate deformylase	0.49	0.046	0.77	0.016
cg1726	*mcmA*	methylmalonyl-CoA mutase, β subunit	0.46	0.010	0.22	0.010
cg1810	*gmk*	guanylate kinase	0.41	0.001	0.86	0.056
cg2558		putative protein related to aldose 1-epimerase	2.12	0.001	1.15	0.226
cg2559	*aceB*	malate synthase	2.24	0.001	2.63	0.005
cg2631	*pcaH*	protocatechuate dioxygenase, β subunit	0.46	0.001	0.33	0.006
cg2836	*sucD*	succinyl-CoA synthetase, α subunit	0.27	0.013	0.35	0.006
cg2837	*sucC*	succinyl-CoA synthetase, β subunit	0.49	0.001	0.35	0.023
		Amino acid biosynthesis				
cg2779	*serB*	phosphoserine phosphatase	0.49	0.001	0.24	0.010
		Cofactor biosynthesis				
cg0095	*bioB*	biotin synthase	0.46	0.011	0.34	0.007
cg0264		putative molybdopterin converting factor, small subunit	2.07	0.001	1.67	0.041
cg1216	*nadA*	quinolinate synthetase	0.35	0.002	0.90	0.137

cg1476	*thiC*	phosphomethylpyrimidine synthase, involved in thiamine biosynthesis	2.47	0.001	8.41	0.001
		Regulation				
cg0986	*amtR*	master regulator of nitrogen control, repressor, TetR-family	2.34	0.049	0.76	0.108
cg2260	*glnK*	nitrogen transcriptional regulator PII	2.23	0.007	0.98	0.256
		Translation				
cg0581	*rpsL*	30S ribosomal protein S12	0.46	0.050	0.56	0.007
cg2791	*rpmJ*	50S ribosomal protein L36	0.45	0.017	0.76	0.214
		Further genes				
cg0241		hypothetical protein, conserved	2.42	0.001	1.27	0.007
cg0439		putative acetyl transferase	2.06	0.010	1.14	0.279
cg0704		conserved protein of unknown function, PFAM Imm68	2.41	0.001	2.15	0.001
cg1252	*fdxC*	ferredoxin	0.29	0.019	0.65	0.021
cg1318		putative DNA repair exonuclease, conserved	2.08	0.009	1.47	0.004
cg1514		putative secreted protein, CGP1 region	2.17	0.022	3.80	0.001
cg1612		putative acetyltransferase	0.37	0.032	0.20	0.009
cg2214		putative Fe-S-cluster redox enzyme	0.48	0.044	0.72	0.184
cg2273	*rncS*	ribonuclease III	2.16	0.002	1.04	0.481
cg2283		hypothetical protein	3.96	0.001	4.38	0.004
cg2285	*hipO*	putative hippurate hydrolase protein	2.07	0.004	0.79	0.118
cg2564		hypothetical protein	3.44	0.007	1.76	0.044
cg2883		putative SAM-dependent methyltransferase	0.20	0.001	0.50	0.003
cg2962		putative heme-degrading monooxygenase	6.46	0.001	12.43	0.005
cg3031		hypothetical protein, conserved	0.37	0.024	0.80	0.005
cg3036	*xthA*	exodeoxyribonuclease III	2.60	0.001	1.31	0.114
cg3423	*trxC*	thioredoxin	2.06	0.004	1.20	0.246